Mutual Gravitational Capture as a Mechanism for Planetary Growth: An Alternative Hypothesis

José Mendes Damian
Independent Researcher, Brazil
ORCID: 0009-0003-7726-1524 - jmdamian@me.com

In this **Version 1 (October 2025),** the results are contextualized according to the velocity parameters involved, and the discussion now presents a more detailed connection among geophysics, geodynamics, and paleobiology, improving:

(i) the clarity through refinements in the explanations of capture dynamics, morphological signatures, and the planetary and biological evolution of Earth;
(ii) the analysis of complete cycles of continental formation and fragmentation, accompanied by recurrent episodes of global warming and cooling;
(iii) the integration of life evolution, correlated with MGC-PC events and environmental transformations over time.

I received valuable comments and additional material, now incorporated into Sections 4.7 and 4.8. The manuscript is the result of 38 years of research, gathering literature and studying models.

Version 0 (Aug 2025) of this manuscript was posted as a non-peer-reviewed preprint on EarthArXiv (https://doi.org/10.31223/X5G451).

ABSTRACT

This study proposes a new hypothesis for the growth of rocky planets through successive events of mutual gravitational capture followed by planetary fusion. The model suggests that collisions resulting from mutual gravitational captures within the Hill sphere occur under initial conditions of zero relative velocity, aligned velocity vectors, and relatively similar mass ratios. Under these parameters, the model predicts that collisions would occur at velocities allowing the complete fusion of the bodies and the formation of structures at multiple scales.

The resulting planetary mass would contain merged inner cores, mantle heterogeneities, mountain chains, continental blocks, and surface redistribution of minerals. Some of these signatures may be associated with magnetic anomalies, hotspots, mantle transition zones, subducted crust, and mass extinction events.

The hypothesis also provides new parameters for simulations of satellite capture and comet ejection during earlier stages, when planets were less massive, enabling testable predictions for future studies on Earth's evolution.

Keywords: life evolution planetary evolution, planetesimals, orbital dynamics, satellite capture, mantle heterogeneities, core evolution, tectonics.

`

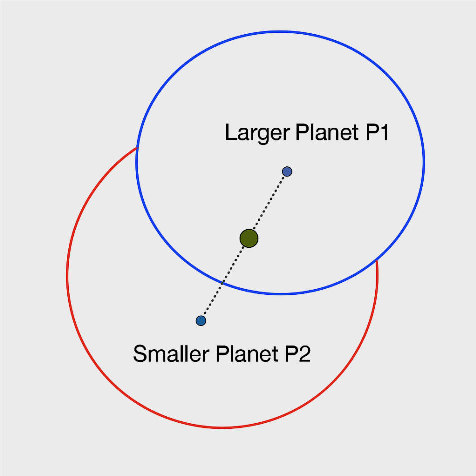

1. Introduction

This study analyzes a particular feature of planetary dynamics that can occur within the Hill sphere: **Mutual Gravitational Capture (MGC)**. In the case of the Solar System, this is a region where the attraction between two bodies exceeds external forces, such as those exerted by the Sun.

In the early Solar System, numerous protoplanets occupied nearby orbits, making their gravitational interactions more frequent. The model investigates a particular aspect of gravitational attraction arising from the proportions of protoplanetary masses that may have characterized one of the evolutionary stages of the inner planets. When the interaction occurred between bodies with large mass differences, it favored satellite capture or ejection within lower-energy regimes.

However, interactions between bodies with less unequal mass ratios favored orbital convergence and eventual merger. In such cases, the impact velocity was primarily determined by mutual gravity, while the orbital velocity vectors became progressively aligned. Thus, mutual gravitational capture could result in **Planetary Coupling (MGC-PC)** that is, the fusion of masses leading to the formation of a new celestial body, leaving long-lasting multidisciplinary evidence across multiple scales.

Classical N-body simulations have successfully described the general architecture of the Solar System, accurately reproducing the proportions of the bodies, orbital angles, velocities, and the energies involved, among other equally relevant factors. However, the convergence of multidisciplinary data suggests that the MGC model may represent an additional mechanism that is relevant to existing models of planetary evolution, particularly in contexts involving internal reorganization and orbital change.

The Giant Impact and Hit-and-Run models explain discrete events such as the Moon's formation (Canup, 2004; Ćuk and Stewart, 2012). Standard accretion models, in contrast, describe planetary growth as a continuous process of accumulation and collisions (Neumann et al., 2024), or as the recurrent formation of planetesimals preserving volatile and isotopic diversity (Chambers, 2004). It should also be noted that the fate of post-impact metals depends strongly on both the thermal state of the target and the presence of a magma ocean (Kendall and Melosh, 2016).

Ipatov (2024), in turn, emphasizes the importance of migration and collisions as structuring mechanisms in the late evolution of planets and satellites. Bizzarro et al. (2025) propose a rapid accretion model that preserves isotopic signatures. Morbidelli et al. (2012) attribute Uranus's extreme axial tilt and the prograde rotation of its regular satellites to successive giant impacts. Crossley et al. (2025) demonstrate that sulfide-rich cores can form in oxidized bodies without the need for extensive silicate melting.

Among the possible agents responsible for mass extinctions is the collision of asteroids, and even the exact timing of the K–Pg extinction event remains challenging. The controversy persists regarding the role of the Chicxulub impact versus possible additional astronomical agents (Renne et al., 2013; Keller, 2012; Keller et al., 2020).

Assuming the feasibility of a successful collision–fusion process, although detailed mathematical verification is still required, the present model advances to interpret enduring morphological signatures widely observed on Earth. These signatures are linked to geophysical transformations, surface reorganizations, and environmental changes that influenced the evolution of life.

The MGC-PC hypothesis proposes a mechanism operating after the initial accretion, involving collisions between differentiated bodies, which allows significant advances in the interpretation of observable evidence, in contrast to slow growth. These fusions would represent an evolutionary stage characterized by mass jumps, with direct implications for internal dynamics, magnetic fields, crustal structure, and even the evolution of biological systems.

The MGC hypothesis engages with the models discussed above while providing multidisciplinary contributions to planetary evolution. It incorporates collisions as structuring mechanisms in the evolutionary process, aligning with models that emphasize gentle instabilities, orbital migration, and systemic reconfigurations. This perspective also helps explain the preservation of deep structural heterogeneities, in line with evidence for partial mergers discussed by Asphaug (2014). Furthermore, it allows for the reinterpretation of persistent magnetic anomalies as possible signatures of deep reorganizations at the core–mantle boundary, considering the sensitivity of the geodynamo to heat flow variations at the CMB, as highlighted by Biggin et al. (2012) and Dannberg et al. (2023).

In this manuscript, we propose a unified physical mechanism developed from an interdisciplinary analysis of data. From this analysis, patterns emerged and progressively structured into hypotheses aimed at explaining the complex cyclic processes that governed planetary evolution under conditions different from those of the present. The article is organized in a logical and progressive manner, through data, patterns, and interdisciplinary connections, culminating in a model still under development. With this model, we seek to reinterpret the referenced multidisciplinary evidence, while acknowledging its validity and the conclusions currently accepted.

This study should be regarded as a conceptual framework that precedes numerical validation. If Mutual Gravitational Capture is indeed a distinct and relevant mechanism compared to conventional collisions, it may not yet have been identified in N-body simulations of the late stages of planetary accretion. Therefore, future detailed modeling — possibly of a hydrodynamic nature — will be required to assess whether, under such conditions, planetary impacts yield outcomes different from those predicted by standard models.

We recognize that, in interpreting the referenced studies individually, especially those from highly specialized fields, some inaccuracies in interpreting the authors' original intentions may have occurred. Nevertheless, we believe that many of these works address aspects potentially compatible with the proposed model. It is, therefore, a model open to continuous revision and an open invitation to constructive engagement.

2. Methodology

Two celestial bodies orbiting their star can interact gravitationally, resulting in a Mutual Gravitational Capture (MGC), which may lead to the following outcomes: (i) the fusion of differentiated bodies through planetary coupling (MGC-PC); (ii) the orbital capture of satellites (MGC-SC); (iii) the ejection of smaller bodies (MGC-CE); or (iv) the formation of bilobed structures. The focus of this study (MGC-PC) is primarily to analyze the enduring morphological signatures, merger dynamics, and resulting orbital effects, considering that collisions between differentiated bodies were common during the evolutionary history of the inner Solar System.

Genda and Abe (2005) state: "*Terrestrial planets formed through gravitational accretion of a large number of planetary bodies (called planetesimals). The final stage of the accretion involved giant impacts between Mars-sized bodies*[4–7]*, and it was during this stage that the primordial atmosphere of the Earth was significantly modified*[8–10]*.*" This planetary formation framework is consistent with the MGC-PC hypothesis, according to which such events occurred frequently on Venus and Earth, as suggested for impacts involving Mars-sized bodies. Extrapolating this reasoning, smaller-scale scenarios may also have involved Mars and Mercury.

2.1. Theoretical Foundations of Mutual Gravitational Capture (MGC)

Mutual Gravitational Capture (MGC) may occur when two planetary bodies enter each other's Hill sphere, a region where their mutual gravitational attraction becomes dominant over external influences, such as that of the Sun.

In this region, their orbital velocities will be similar, allowing capture if mutual attraction overcomes their respective inertia. Otherwise, the interaction will result only in an orbital deflection, after which both bodies will continue on separate trajectories.

When capture occurs, mutual gravity gradually reduces both the distance and the orbital velocity difference between the bodies, while increasing their relative approach velocity. The final impact speed is governed primarily by mutual gravity. Energy is dissipated mainly in the core and mantle, with additional contributions from crustal deformation, the atmosphere and the oceans.

Based on these parameters, we adopted a conservative energy dissipation rate of 20%. Genda and Abe (2005), although not providing a direct numerical value, demonstrate that oceans amplify atmospheric loss and rapidly convert impact energy into vapor, thereby increasing dissipation. Without explicitly stating the rate, Collins et al. (2012) describe how impact energy is redistributed among heating, deformation, material ejection, and geochemical processes.

We also considered additional factors during the approach of the bodies, such as the convergence of orbital velocity vectors, which reduces the impact angle, and the progressive intensification of tidal forces. Moreover, parameters such as mass ratio and relative positioning (i.e., whether the more massive body leads or follows) also influence the orbital dynamics of the process.

Critical velocity and planetary fusion: According to Genda et al. (2012): "$v_{(cr)}/v_{(esc)}$ *increases with decreasing impact angle or mass ratio, which means that collisions with low* *impact angles or low mass ratios tend to be merging events.*" The authors indicate that successful merging occurs in collisions below the critical velocity, which itself may exceed the system's escape velocity. In their model, the critical velocity depends on the mass ratio *(γ)*, the impact angle *(θ)*, and empirical coefficients *(c_1–c_5)* derived from hydrodynamic simulations (see Eq. (1) in Genda et al., 2012).

In the absence of energy dissipation *(η = 1)* and initial relative velocity, the model show that the head-on impact velocity corresponds to the escape velocity of the binary system *(v_{impact} = v_{esc}):*

$$v_{impact} = \sqrt{\eta\left(\frac{2GM_1}{r_{impact}} + \frac{2GM_2}{r_{impact}}\right)} \quad = \quad v_{impact} = \sqrt{\frac{2\eta G(M_1 + M_2)}{r_{impact}}}$$

$$v_{esc} = \sqrt{\frac{2G(M_1 + M_2)}{R_1 + R_2}} \quad = \quad v_{esc} = \sqrt{\frac{2G(M_1 + M_2)}{r_{impact}}}$$

Other key equations used in the theoretical framework include relative kinetic energy: $E_k = \frac{1}{2}\mu v_{rel}^2$, Hill limit (maximum distance of gravitational influence): $\mathrm{d_H} = a\left(\frac{M}{3M_\odot}\right)^{1/3}$

The Roche limit corresponds to the minimum distance at which non-rigid bodies with similar densities can approach another without the near side of the smaller body breaking apart: $dR = 2.44R_M$.

Studies suggest that head-on impacts tend to be more destructive than low- to moderate-angle impacts *(<45°)* and that, depending on the mass ratio, they may result in either body complete fusion or grazing encounters (Genda and Abe, 2005; Genda et al., 2012; Kegerreis et al., 2020; Denman et al., 2022). At higher angles (≥45°), hit-and-run events become common, with the impactor potentially escaping the system entirely in collisions with *θ > 60°*, as supported by several recent studies (Emsenhuber and Asphaug, 2019; Emsenhuber et al., 2020; Asphaug et al., 2006).

Denman et al. (2022) demonstrated that collisions between super-Earths are favored at low impact angle and velocities, allowing for complete merging and the formation of a single planet. The authors further state that in such collisions, the cores of the two planets meet and combine at the gravitational center of the new body, forming a single unified core. They conclude that part of the mantle may be ejected, while the remaining material is redistributed around the combined core.

Studies indicate that it may have been common for protoplanets to adjust their orbits during migration and temporarily enter mutual resonances, even sharing nearby orbits and establishing a transient co-orbital regime (Raymond et al., 2020; Raymond, 2024). Canup and Asphaug (2001) indicate that oblique impacts between nearly formed planetary bodies can generate stable orbital disks, such as the one that may have given rise to the Moon, even without complete merging or total destruction. Additional studies suggest that moderate collisions may lead to partial mergers and bilobed structures in undifferentiated bodies, such as certain asteroids and comets (Jutzi and Benz, 2016; Hu et al., 2018; Zhao et al., 2015).

2.2. Hypothesis and Modeling

Complementing studies that assume pre-existing impact velocities, the MGC-PC hypothesis proposes a specific physical mechanism responsible for collision speeds: mutual gravitational attraction between bodies in nearby orbits. In this context, the impact velocity is naturally regulated by the gravitational attraction of the system's total mass, since the difference in orbital velocity between the bodies tends toward zero at the moment of impact. Thus, the model focuses on MGC-PC outcomes, in which coalescence between the bodies may be favored.

The model considered three scenarios to evaluate the feasibility of collision, mass fusion, and the resulting morphological signatures (Table 1). However, Scenario III is not modeled here, as it involves collisions driven by pre-existing orbital trajectories rather than convergence governed by mutual gravitational attraction—a central condition of the MGC-PC framework.

Table 1. Comparative scenarios for planetary capture and fusion

Scenario	Initial configuration	Main dynamics	Typical outcome
(i) External	Outer body slower behind (chaser)	Outer body pulled inward, inner body pulled outward, with favorable rotation	Near-frontal angle, impact velocities near critical threshold
(ii) Internal	Inner body faster ahead (chaser)	Same as scenario (i), with opposite rotation	Similar to external, with opposite rotation
(iii) Direct	Orbital velocities and trajectories	High-energy collisions, material dispersal	Impacts with combined orbital and gravitational velocity

Scenario I: A collision occurs when the impactor follows an external orbit, with the orbital velocity difference between the bodies approaching zero at the moment of impact. The bodies follow nearby elliptical orbits, so that mutual gravitational attraction gradually aligns their orbital direction and velocity vectors, resulting in an impact angle tending toward a head-on geometry. The collision increases the total angular momentum, intensifying the rotation of the New Planet. The resulting merged mass tends to follow the average direction of the orbital vectors of the colliding bodies, favoring coalescence and reducing dispersion.

Scenario II: A collision on the inner side under the same conditions as Scenario I, but with an impact vector opposite to the rotation, thereby subtracting angular momentum. This may cause a deceleration or even a reversal of rotation.

The order of approach, namely, which body leads based on the mass ratio, influences the relative impact velocity, while the impact point determines the resulting obliquity. Different combinations of planetary rotation directons can produce complex effects. The modeled process is summarized in Figure 1, which illustrates the stages from orbital approach to structural reorganization of the planet.

2.3. Application of the Model to the Formation of the Earth

Earth was chosen as the reference model due to its greater mass among the inner planets and the availability of multidisciplinary evidence for both the approach and merger phases. The model considers:

(i) Variable mass proportions between planetary bodies: Mass ratios between 40% and 60% of the resulting total mass are considered, representing the smaller and larger bodies, respectively;

(ii) Gradual orbital convergence, with the orbital velocity difference between the planets, decreasing and tending toward zero;

(iii) Relative impact velocity calculated to be based exclusively on mutual gravitational attraction, initially disregarding the small orbital velocity difference at the moment of collision;

(iv) Impact angle: assumed very close to be zero, which reduces the critical velocity required (a worst-case scenario for coalescence), although a very low angle is expected due to the approach being governed almost exclusively by mutual gravitational attraction. This assumption was adopted to test the lower limit for coalescence. It is recognized that moderate angles (~30° to ~45°) are more favorable for merging, and that this is a conceptual simplification;

(v) However, it is acknowledged that this residual orbital difference and a moderate impact angle (up to ~45°) may exist and could be incorporated into future simulations without significantly altering the expected outcomes.

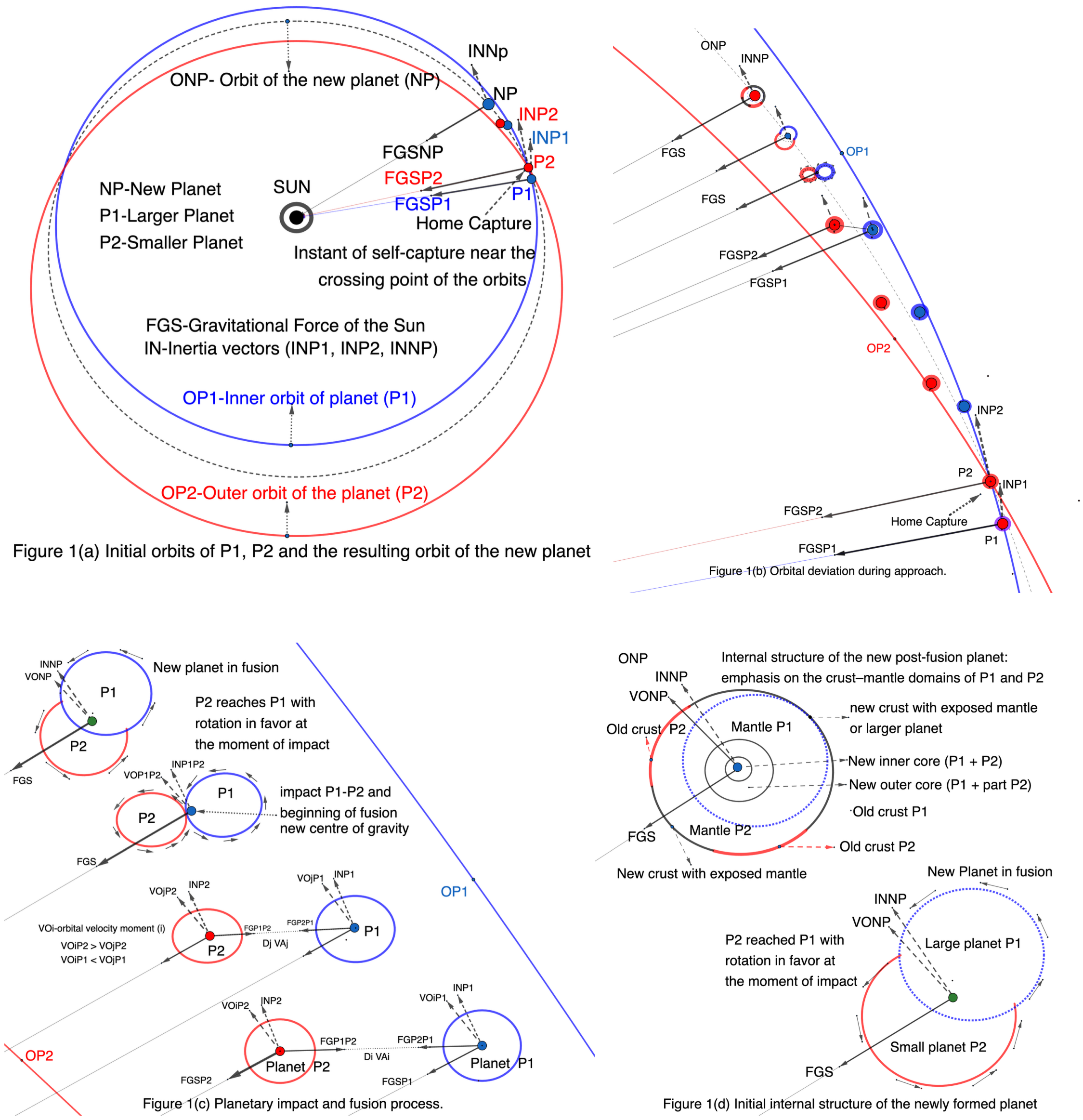

Figure 1(a) Initial orbits of P1, P2 and the resulting orbit of the new planet

Figure 1(b) Orbital deviation during approach.

Figure 1(c) Planetary impact and fusion process.

Figure 1(d) Initial internal structure of the newly formed planet

3. Results: Parameter Analysis, Planetary Merging, and Morphological Modeling

Computational simulations are powerful tools for projecting past or future scenarios, allowing the development of mathematical models consistent with physical observations. The rigor of such models depends strongly on the input parameters, which must represent known empirical evidence while also allowing additional variables capable of capturing phenomena not yet observed.

In this context, we evaluated impact velocities in hypothetical events of Mutual Gravitational Capture with Planetary Fusion (MGC-PC), which may provide new insights into stages preceding the formation of the present-day inner planets of the Solar System.

3.1. Feasibility and Model Parameters

`

In this subsection, we assess the physical feasibility of the MGC-PC model based on orbital parameters, impact velocities, and stability tests. This process, although applied here to smaller bodies such as Earth, shows partial similarities with the results of Denman et al. (2022), obtained for collisions between super-Earths.

Among the inner planets, average orbital velocities range from 47.9 km/s (Mercury) to 17.9 km/s (Ceres). For modeling purposes, we considered head-on collisions between bodies with mass ratios between 40% and 60%, initially assuming that both had similar orbital velocities at the moment of impact. This is a significant simplification and represents a recognized limitation of the model, as small differences in orbital velocity are expected. However, we acknowledge that modest variations in relative velocity and impact angle are possible, depending on the mass ratio and which body leads the orbital trajectory during the approach.

Impact Velocity Results: In our modeling, assuming no initial relative velocity and without considering energy dissipation, such collisions would generate impact velocities, driven by mutual gravitational attraction, ranging from 3.37 km/s (Mercury) to 8.79 km/s (Earth).

According to Genda et al. (2012), in head-on collisions *($\theta = 0°$)*, the impact velocity corresponds to the escape velocity of the system, whereas the critical velocity for merging may exceed the escape velocity depending on the mass ratio and impact angle. For mass ratios close to 1, the critical velocity is greater than the system's escape velocity, that is, $v_{impact} \approx v_{esc} < v_{crit}$. This critical threshold may increase further as the mass ratio deviates from unity or as the impact angle becomes moderate. This range supports the physical feasibility of planetary merging in a scenario that considers the worst case (head-on collision) and the best case (no difference in orbital velocity between the bodies immediately before impact). Thus, there is room for a moderate increase in impact angle and for small relative velocity differences at the moment of collision.

Considering an energy dissipation of up to 20%, the estimated values remain well below the critical threshold for a successful collision. The value may vary slightly, depending on the impact geometry, energy dissipation, or collision angle.

These estimates are preliminary, based on conceptual simplifications, and require detailed numerical modeling to more accurately quantify fusion thresholds under varying impact conditions and compositions, as discussed in Section 4.10.

Stability and Sensitivity Tests: Figure 4 presents a simulation of a complete cycle of the MGC-PC model, involving successive planetary fusion events and showing stepwise growth of mass, surface area, and gravitational acceleration, demonstrating the model's internal consistency. Variations in the mass ratio between 40% and 60% result in nearly overlapping velocity curves, indicating stability even with significant differences between the bodies. Future studies, preferably using hydrodynamic simulations, may refine these limits and assess the conditions under which the MGC-PC hypothesis remains valid.

3.2. Approach phase to impact

Capture begins at some point within the Hill sphere, when mutual attraction overcomes relative inertia and the bodies start progressively approaching, evolving into a planetary coupling event (MGC-PC). In this cases, pre-existing satellites may be relocated, ejected, or absorbed by the resulting planetary mass.

Approach and gravitational deformation: As the bodies draw closer, their gravitational centers shift forward, deforming them into ellipsoidal shapes. Tidal forces intensify, accelerating the relative approach velocity and, beyond a certain distance, uplifting the crusts.

Upon reaching the Roche limit, the frontal crust of the smaller planet ruptures, while its opposite face preserves ancient cratons with geological records. The proportion of preserved crust is a hypothesis that remains to be tested through geochemical studies and impact modeling at velocities below the critical threshold. At this stage, loose materials such as water and atmosphere gases migrate toward the displaced center of gravity in the impact region. At the moment of impact, the prominent crust of the larger, slightly ellipsoidal planet comes into contact with the fractured frontal face of the smaller planet, possibly striking its mantle directly, in an environment potentially covered by oceanic waters.

According to the Borsuk–Ulam theorem, on any sphere there exist two antipodal points sharing a common property. This symmetry may provide a mathematical basis for interpreting crustal weakening observed on the side opposite the impact. The application of this concept is exploratory and remains subject to future validation.

Genda and Abe (2005) show that terrestrial planets formed through the accretion of planetesimals, giving rise to dozens of Mars-sized protoplanets that collided with each other. These impacts generate shock waves that travel through the planet and affect the antipodal region of the impact site. They estimate that collisions between similar-sized bodies can result in up to 30% atmospheric loss. For modeling purposes, they assumed that all protoplanets near Earth's orbit possessed oceans during this phase.

The collision generates an asymmetric mass with a displaced center of gravity, initially located near the point of contact (Figure 1(c)); but within the larger body. Although applied here to differentiated bodies, this configuration resembles the bilobate structures observed in comets and asteroids, such as 67P/Churyumov-Gerasimenko and 4179 Toutatis.

Loose Material Dynamics: The displaced gravitational center redistributes loose materials, water, sediments, and gases, creating what we refer to here as the *Hydrobiological Ring*, a conceptual illustration used to describe the transient concentration of these materials at the impact interface. The intense displacement of water, far greater than typical megatsunamis, would be recorded in the continental crust.

As the merger progresses, the center of gravity shifts and the new mass tends toward sphericity, while the larger planet becomes covered by a layer of the smaller body's mantle mixed with its own liquid core. At the contact between the original planet and this overlying mantle, an asymmetric interface zone develops, with significantly greater depth on the opposite side (Figure 1(d)). In this zone, a large portion of the Hydrobiological Ring material is trapped, where reactions occur between the mantle, the crust, the water, and other ring components, including biological matter.

The remaining ring material is redistributed over the expanding surface, flowing across the continents and newly exposed mantle areas. On the continents, water and these material accumulate in basins that become covered by sediments. On the newly exposed surfaces, the water undergoes intense evaporation, forming salt layers whose vapors mix with gases and ash. This process raises the temperature of the waters, creating a warm and acidic marine environment, and also triggers intense and prolonged rainfall. In this context, if present in sufficient quantity, water cools the magma and supports the continuation of life; otherwise, it may result in an acidic atmosphere.

The new environment will exhibit an expanded surface that alters the hydrological balance and sea level, as well as distinct chemical composition and climatic patterns. The process is fatal to living organisms, and the dynamics of the waters tend to concentrate organic matter in specific regions. These include the deep mantle, continental basins, and the ocean floor (beneath layers of sediment or salt), as well as polar regions where thick ice sheets later form.

Preserved and newly formed crust: Upon impact, the preserved crust of the smaller planet fragments into continental blocks that float upon the mantle of the larger planet. These blocks move in seemingly random and independent patterns, guided by gravitational and rotational flows, moving as if riding a wave. This mantle initially spreads out, drawn toward the center of gravity, which shifts as the New Planet becomes more spherical.

New surfaces emerge between the moving continents, formed by lighter materials from the mantle. Initially, materials denser than the upper crust but still lighter than those that will later rise come to the surface, potentially creating elevated regions at the zones of separation, as if forming magmatic ridges.

During continental drift, the leading edges of the continental blocks push magma ahead of them, because to their smaller curvature relative to the planetary mass. As the blocks move apart, they develop fractures in decreasing scales of length and width, forming a network of progressively smaller microfractures that adjust their curvature to accommodate the New Planetary volume. The first curvature adjustment raises continental topography, forces mantle upwelling, and may result in the formation of mountain belts along the leading edges.

3.3. Formation and final structure of the New Planet

After the merger, an adjustment phase begins to equalize the thickness and composition of the internal layers. Less dense materials from the larger body tend to rise, while denser materials from the smaller body, including its core, migrate toward the system's center of mass.

The larger body becomes covered by a variably thick layer composed of material from the smaller body, forming an interface zone (Figure 1(d)). This layer thickens on the side opposite the impact, while the original crust of the larger planet may remain exposed at the impact site, depending on the secondary body's volume.

Increasing internal density, pressure, and temperature favor the migration of solid cores toward the center of mass. Initially, the inner core may consist of juxtaposed solid spheres that could gradually fuse, depending on pressure, temperature, and composition. During this migration of the inner core, a low-pressure zone forms, attracting part of the outer core of the smaller body, including water and volatiles. Another portion of the outer core mixes with its own mantle, either homogeneously or heterogeneously.

The internal layers restructure according to density, establishing a new equilibrium for rotation rates, including possible differential rotation among the inner spheres if they do not merge.

This event also alters the orbit, axial tilt, and other aspects of planetary motions, influenced by the proportions of the merged masses, solar gravity, and the action of satellites. The precession of the equinoxes changes drastically, reflecting the new gravitational configuration and the absence of the previously nearby body.

The resulting surface combines three distinct regions: preserved crust fragmented into continental blocks, newly formed crust creating elongated basins between them; and a large plain at the impact site, where part of the larger planet's crust may remain exposed. This large plain will have a semicircular shape with elevated edges, resembling a shallow crater or basin, resulting from the displacement of the smaller body's mantle under the influence of gravity, rotation, and interaction with water. For bodies with similar densities, the preserved crust of the smaller planet may account for up to 32% of the new surface. After the surface of the new mass solidifies, new tectonic plates are expected to form.

Assuming equal densities, the New Planet would have a surface area approximately 60% larger than that of the smaller planet. If about 50% of the smaller planet's crust is preserved and fragmented into continental blocks, the continental surface of the New Planet could represent nearly one third of its total area. The remainder would consist of new, lower-lying regions with exposed magma. One of these newly formed areas will likely include plains between the diverging continental blocks, while at the impact site, the configuration will depend on the volume ratio between the bodies.

In the final stages, the expanding mantle gradually ceases motion under the influence of gravity, rotation, and water interaction. This process can produce semicircular regions of varying sizes, where the crust of the larger planet remains exposed and surrounded by elevated edges. In addition, immediate extinctions and those resulting from lack of adaptability are followed by the emergence of survivors in a new habitat. In this context, plants, aquatic ecosystems, certain niches, and resilient, adaptable species can persist.

Figure 2 illustrates the stages of planetary coupling (MGC-PC), while Figure 3 shows the resulting morphological features. These are reinterpreted in light of the MGC-PC hypothesis in the following sections: Geophysics and Geodynamics; Structural Geology; Geochemistry and Mineralogy; Paleontology; and Astronomy and Astrobiology.

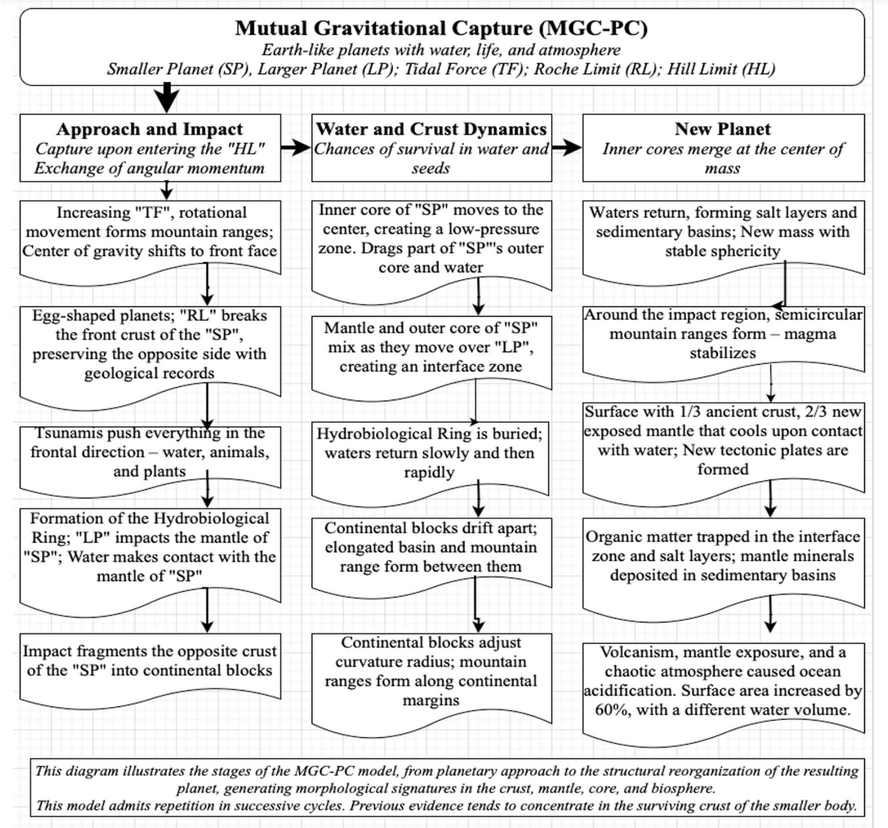

Figure 2 – Steps of the MGC-PC process resulting from Mutual Gravitational Capture (MGC).

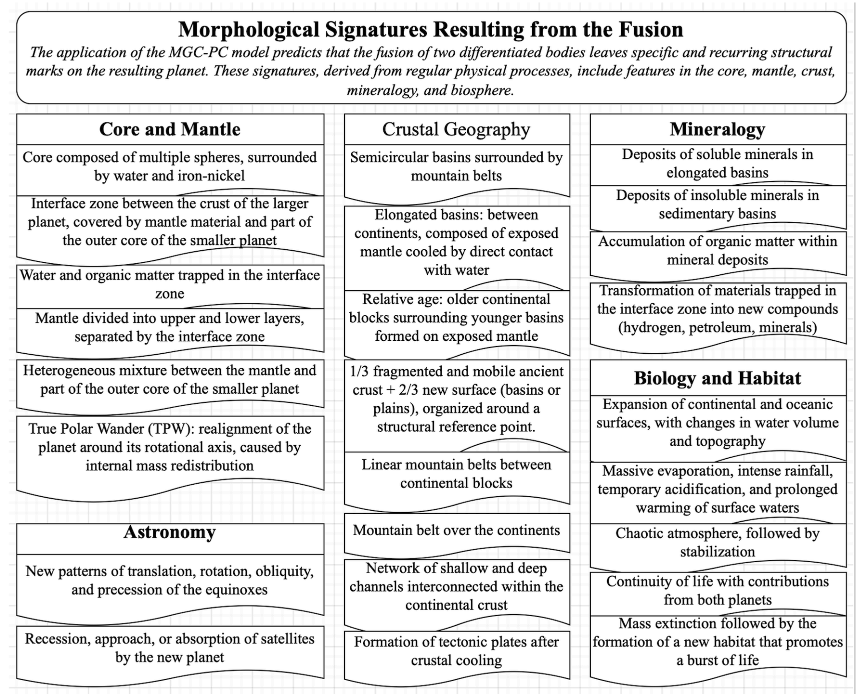

Figure 3 – Persistent morphological signatures generated by the MGC process

4. Discussion

According to Genda et al. (2012), the inner planets formed from collisions among dozens of protoplanets with sizes comparable to Mars. The present hypothesis predicts collisions tending toward head-on on geometry, with impact velocities determined predominantly by mutual gravitational attraction and only marginally influenced by differences in orbital velocities. The impact severity is directly related to the masses involved and approximately equals to the system's escape velocity. Under these conditions, impact velocities remain below the fragmentation threshold proposed by Genda et al. (2012), further reduced by energy dissipation. The main remaining uncertainty concerns the effective contribution of residual orbital velocity differences, even when the motion vectors are aligned in the same direction.

The enduring morphological signatures proposed by the model will be correlated with empirical evidence reported in the literature and reinterpreted in light of the MGC-PC hypothesis in the following sections:

(i) Sections 4.1 and 4.2: ULVZs, LLSVPs, transition zone, hotspots, SAMA, and other mantle heterogeneities;
(ii) Sections 4.3 and 4.4: mountain uplift, crustal fragmentation, and reorganization;
(iii) Section 4.5: water–mantle interaction, surface minerals, and petroleum;
(iv) Sections 4.6: fossil and sedimentary records and mass extinctions.

In Sections 4.7, 4.8, and 4.9, the model will be applied to the evolution of life and inner bodies, as well as to the formation of satellites and comets.

The model is conceptually applied to planetary coupling cycles, deep geophysical and geochemical signatures, parallels in other planets, and contrasts with existing models. Finally, Section 4.10 presents the methodological limitations and simplifications of the hypothesis.

4.1. Geophysics of the New Planet: Core and Magnetic Anomalies

The MGC-PC process proposes that the fusion of differentiated bodies reorganizes the core, mantle, and crust, favoring the migration of multiple inner cores toward the new center of mass. The movement of the inner core creates low-pressure zones that attracted volatile and viscous materials, including water, toward the center of mass.

This process may result in an inner core composed of several solid spheres surrounded by metallic liquids and volatiles, rotating independently if the cores do not fully merge. However, this dynamic state may gradually evolve toward unified rotation as the body stabilizes its total angular momentum.

The core is surrounded by the outer core, composed of iron and nickel, and contains high concentrations of sulfur (Savage et al., 2015). Seismological observations reveal physical heterogeneities, anisotropies, rotational variations, and structural changes in the shape and composition of the inner core (Wang et al., 2024; Vidale et al., 2025; Mäkinen and Deuss, 2011), incompatible with the view of a single, homogeneous, and static body. He et al. (2022) state: "*The Earth's inner core (IC) is less dense than pure iron, indicating the presence of light elements within it. Silicon, sulfur, carbon, oxygen, and hydrogen have been suggested as possible candidates*."

Deuss (2014) shows that the upper 60–80 km of the inner core appears isotropic, while the central region is anisotropic, with seismic waves propagating faster along the polar direction. Zhou et al. (2022) show that the geomagnetic field was very weak around 565 Ma, increasing rapidly after 550 Ma, coinciding with the probable growth of the inner core to ~50% of its current radius by 450 Ma.

The MGC-PC hypothesis suggests that, in addition to the inner core doubling in size with each successive event, internal pressure increases significantly. This favors physicochemical interactions and the migration of dispersed mantle iron toward the center, contributing to the progressive growth of the inner core. Consequently, the inner core would consist of the original solid cores, complemented by volatiles filling the spaces between these spheres, possibly solidified at a later stage. This approach provides a new physical basis for interpreting the observed heterogeneities, supporting the need to revise the conception of the inner core as a solid, homogeneous, and static body. In addition, it suggests that surface gravity may also change as a function of mass increasingly concentrated in the inner core.

4.2. Geophysics of the New Planet: mantle heterogeneity

The MGC-PC model suggests that the mantle of the smaller planet mixed with part of its outer core and spread across the larger planet, possibly generating heterogeneities consistent with seismic, geochemical, and thermal anomalies observed in Earth's mantle today. At the contact between this layer and the original crust of the larger planet, an interface zone developed, significantly deeper on the side opposite the impact (Figure 1 (d)). This zone may extend from the surface, through the transition zone, down to the Gutenberg discontinuity, trapping water, organic matter, and other volatiles capable of generating hydrogen and hydrocarbons under high pressure. Studies indicate the existence of water oceans in the mantle transition zone, retained within minerals (Pearson et al., 2014; Gu et al., 2022; Huang et al., 2005; Hallis et al., 2015). Calcium-rich rocks have been identified below 300 km depth (Brenker et al., 2005).

Other heterogeneities include the South Atlantic Magnetic Anomaly (SAMA) (Finlay et al., 2020) and hotspot regions, encompassing moderate heterogeneities such as the Yellowstone supervolcano, characterized by its sulfurous waters and yellowish rocks (Nordstrom et al., 2009). These heterogeneities may represent mixtures of mantle and outer-core material, which is consistent with the high sulfur concentration in the outer core (Savage et al., 2015).

During this process, the inner core of the smaller planet migrates toward the new common gravitational center from the side opposite the impact location. Along this path, it may drag volatile materials, such as water and liquid iron-nickel. Part of this flow may form persistent compositional bubbles in the mantle, potentially linked to the SAMA.

The buried crust of the larger planet, initially continuous, may fragment into blocks of different sizes (small, medium, or large), creating deep heterogeneities. Consequently, this crust became covered by mantle material through a process distinct from the subduction described by plate tectonics, potentially explaining the formation of structures such as LLSVPs and ULVZs (Biggin et al., 2012; Dannberg et al., 2023; Hansen et al., 2023; Yuan et al., 2023; Wang et al., 2024; Feng et al., 2021; Torsvik et al., 2016). Numerical models also indicate that thermal plumes can entrain dense layers from the lower mantle into shallower regions, preserving deep heterogeneities (Zhong and Hager, 2003).

Between 320 and 200 Ma and during the last 80 Ma, van Hinsbergen et al. (2021) show that major tectonic reorganizations, including the initiation of subduction, may be triggered by deep mantle plumes without prior collisions or pre-existing convergent boundaries. Messling et al. (2025) identified positive ε^{100}Ru anomalies and negative μ^{182}W signatures in modern basalts from Hawaii, Greenland, Africa, and Germany, concluding that outer core material was incorporated into the deep mantle during the first ~60 million years of the Solar System.

Additional studies support the hypothesis of crustal burial and mantle-core mixing during successive planetary fusion cycles. Dannberg et al. (2023) indicate that thermal heterogeneities at the core-mantle boundary (CMB) evolve cyclically with the formation and breakup of supercontinents, generating deep structural anomalies that affect the planet's thermal and magnetic dynamics. Small zircon populations dated between 165 Ma and 2.5 Ga (Rojas-Agramonte et al., 2024, 2022; Greenough et al., 2021) and magnetic signatures preserved in iron-rich minerals within the transition zone (Kupenko et al., 2019) reinforce this scenario.

In the context of the MGC-PC model, the continents move together with the mantle of the smaller planet as it spreads over the larger one. Analogously, Vaes and van Hinsbergen (2025) describe True Polar Wander (TPW) as the simultaneous motion of the crust and mantle relative to the rotation axis.

The literature has described these mantle heterogeneities in detail, interpreting them appropriately within current models. However, when considered together—particularly including LLSVPs, ULVZs, CMB variations, LIPs, hotspots, plumes, TPW records, and evidence of buried water—these observations show remarkable compatibility with the effects predicted for MGC-PC events. This model proposes that the mantle and continents of the smaller body spread over the larger planet, burying volatiles, while part of its outer core is heterogeneously mixed into the mantle. The result is the formation of a layer of variable thickness that covers the larger planet, as illustrated in Figure 1(c).

4.3. Structural Geology, Paleogeography, and Tectonics: Orogenic Processes

Recent orogenic belts suggest that an MGC-PC event occurred around 66 Ma, which may serve as morphological markers of the MGC-PC cycles (Section 4.8), expressed through four main mechanisms:

(i) structures associated with the ancient subduction zone of the larger planet (Ring of Fire);
(ii) magma release at the onset of continental rifting (Mid-Ocean Ridges);
(iii) crustal uplift driven by tidal forces (Alpine–Himalayan orogeny);
(iv) curvature adjustment along continental margins (Andean belt).

The Ring of Fire may represent the boundary of the ancient subduction zone of the larger planet, with crust exposed within its perimeter. Mid-ocean ridges may have resulted from the initial upwelling of low-density magma, exposed during the first drift of continental blocks. The rapid uplift of the Andes, recorded as abrupt between 10 and 6 Ma (Hoke and Garzione, 2008), is consistent with the curvature adjustment proposed by the MGC-PC model.

Strong tidal forces during planetary approach, before reaching the Roche limit, could have uplifted the crust and formed the Alpine–Himalayan structure. Some au,thors describe its evolution in four distinct phases over the past 66 Ma (Valdiya, 1984), while others place the main collision between ~55 and 50 Ma (Rowley, 1996). Jagoutz (2019) interprets the changes in the Kohistan–Ladakh arc at ~50 Ma as a product of the India–Asia collision. In the MGC-PC model, these changes would be a consequence of tidal forces associated with planetary coupling at ~66 Ma, which displaced India toward the Himalayas and triggered orogenic uplift prior to the full collision.

4.4. Structural Geology, Paleogeography, and Tectonics: Crustal Restructuring and Geodynamic Implications

The crust of the New Planet results from young surfaces formed by exposed magma, portions of the larger planet's crust, and blocks from the smaller planet's crust. The latter initially forms a temporary supercontinent, which subsequently fragments into continental blocks. On present-day Earth, the North Pacific may indicate the impact point of the final event, while the southern region of Africa, at the antipode, may reflect an area of weakened crust. It should be noted that young areas can be continuously rejuvenated when located near divergent boundaries, due to the continuous upwelling of magma, as occurs along the Mid-Atlantic Ridges.

Supercontinent cycle: Studies suggest that the supercontinent cycle may be related to changes in mantle flow, core dynamics, volcanism, and environmental disturbances. Furthermore, there is a need for an approach that incorporates deep crustal restructuring and non-conventional internal processes (Nance et al., 2019, 2014). Pastor-Galán et al. (2019) link the formation and breakup of supercontinents to environmental changes and variations in Earth's magnetic field. Studies suggest that the assembly and breakup of Rodinia (~750 Ma) and Pannotia (~550 Ma) followed these patterns (Nance et al., 2019; Bond et al., 1984).

In this context, the MGC-PC hypothesis offers an alternative framework: it proposes that the planetary surface may expand significantly during fusion events that preserve part of the smaller planet's crust. This crust becomes fragmented into new continents that move independently of conventional tectonic plates and may experience differential subsidence. After the formation of new tectonic plates, divergent movements and volcanism continuously bring mantle material to the surface, rejuvenating it. Examples of subsidence include Greater Adria, which was almost entirely subducted and incorporated into the Alpine orogens (van Hinsbergen et al., 2019), and Zealandia, a submerged and fragmented continent.

Supercontinent reconstruction: The MGC-PC model suggests that, assuming equal densities and an idealized spherical shape, the New Planet would have approximately one-third of its surface composed of preserved crust from the smaller planet—a value close to the current continental area of Earth (~29%). Retroactively reconstructing past continents is complex, as it depends on the volume of water present during each evolutionary stage of the smaller planet (see Section 4.8). The reconstruction process involves removing low-lying regions and rescaling the globe until the remaining blocks cover about 50% of the surface, then repeating the procedure for the previous stage. It is important to observe the cratons and examine the orogenic belts in detail.

4.5. Geochemistry and Mineralogy: Petroleum and Mineral Reserves

The MGC-PC hypothesis proposes that, during planetary fusion events, large volumes of water interacted abruptly with the mantle and the outer core of the smaller planet, burying part of this water along, with organic matter under, under extreme temperature and pressure conditions.

Fate of extinct organic matter: The organic material from mass extinctions, together with water, may have been buried in deep mantle zones at the interface between the colliding bodies (Figure 1 (d)). These zones may have encompassed extensive portions of the larger planet's ecosystem. Organic matter could be transported by water and accumulated in continental or oceanic basins beneath layers of sediment containing salt, which acts as a natural catalyst. In the polar regions, in turn, organic compounds would be covered by an ice layer.

In such environments, organic matter would remain immobilized for extended intervals under high pressure and temperature, in contact with saline waters and reactive rocks. This combination may have generated chemical and mineral heterogeneities, favoring the formation of hydrogen, hydrocarbons, (including methane and other gases) trapped at various depths. Research indicates methane leakage on the seafloor of Antarctica (Seabrook et al., 2025). It is also possible that pre-existing petroleum reserves in the crust of the larger planet were preserved almost intact in the deep mantle during planetary fusion.

Such environments may have favored the generation of hydrocarbons consistent with both biogenic and abiogenic models (Sleep et al., 2012). This perspective helps explain the reserves now found in continental regions corresponding to former inland seas or marine environments (Li et al., 2019; Hein and Cotterill, 2006; Konyuhov and Maleki, 2006), including those extending into the deep mantle (Kutcherov and Krayushkin, 2010). Höök et al. (2010) evaluated both scenarios and found stronger empirical support for a biogenic origin.

Minerals: The MGC-PC events may have promoted the direct contact between ocean water and the exposed mantle. Pressure and thermal shock may have enabled the ionization of part of the semi-molten mantle minerals, allowing their transport in solution around the planet. In this state, the elements would tend to group by affinities, with some precipitating more rapidly, while others would remain in solution for longer, depending on specific conditions for precipitation. Due to these affinities, compatible elements are deposited together or in relative proximity. Particles of organic matter and other components, in addition to contributing to the process, may have precipitated together with these minerals. Thus, ancient seas or oceans are expected to contain significant concentrations of these minerals, buried beneath sediment layers associated with MGC-PC events. Future studies may decipher the ideal conditions for the precipitation of ions suspended in ocean waters, such as pH, temperature, and depth, as well as the temporal intervals and the thickness of the sedimentary layers covering these deposits.

Evidence from Fischer-Gödde et al. (2024), Fouquet et al. (1988), Javoy and Kaminski (2014), and Berezhnaya and Dubinin (2017) confirms the presence of metals in seawater and in continental deposits, even in places without signs of volcanism or hydrothermal activity, which were formerly ocean floors.

4.6. Paleontology: Extinctions, Fossils and Sedimentary Rocks

The so-called “Cambrian Explosion” is well supported by multiple fossil records and represents a rapid, multifactorial diversification not attributable to a single cause (Zhang and Shu, 2013). Montañez (2022) indicates that faunal and floral reorganizations may have occurred in the late Paleozoic.

Large igneous provinces (LIPs) show recurrent correlations with environmental crises over the past ~260 million years, although in some intervals, episodes of oceanic anoxia appear more closely linked to biodiversity loss than to global mass extinctions (Courtillot et al., 2003). Other studies suggest that diversification and extinction were not uniform across space and time (Long et al., 2025).

In the Late Cretaceous of North America, the apparent decline of dinosaurs reflects reduced detectability in the fossil record, while modeled habitat occupancy remained stable (Dean et al., 2025). Brusatte et al. (2015) associate the K–Pg extinction with the Chicxulub impact and Deccan volcanism. However, the Chicxulub crater remains controversial, with offsets of tens to hundreds of thousands of years between the meteorite impact and the peaks of extinction or acidification. For this reason, the hypothesis of a second impact was considered but later discarded (Renne et al., 2013; Keller, 2012; Keller et al., 2020).

Other studies suggest that mass extinctions coincide with abrupt changes in climate and sea level (Barrera and Savin, 1999). Studies indicate that a fully erect neck posture in sauropods would have been physiologically improbable (Seymour & Lillywhite, 2000, 2016; Snelling & Seymour, 2024; Seymour, 2016, 2009).

We consider that MGC-PC events introduce new insights into the study of environmental crises such as destabilizing the crust, exposing the mantle, and releasing large volumes of volatiles into the atmosphere. This would represent a cyclical process capable of generating long-lasting morphological signatures in geophysics and planetary physical geography. In this hypothesis, planetary conditions (effective mass, continental configuration, and oceanic volumes) would have provided a habitat distinct from the present for the evolution of life. In each event, survival would have favored aquatic organisms or those protected in isolated niches on both colliding celestial bodies.

Fossils and Sedimentary Rocks: These records provide valuable evidence of climate cycles, gravitational variations, and orbital dynamics throughout each geological period. Climatic and astronomical patterns, such as solar and precessional cycles, are preserved in laminated rocks that record glacial melting (varves), found across different regions and time intervals. Tidal cycles are captured in sedimentary formations known as tidal rhythmites, while shell fossils from mollusks and other shelled organisms document daily growth increments that reflect ancient day–night cycles.

Evidence from these records indicates that an Earth year once consisted of between 435 and 369 days (Williams, 2000; Mazumder, 2004; Williams, 1998; Poços, 1963; Scrutton, 1978; de Winter, 2020). Collectively, these data provide the empirical foundation for linking geological and biological transformations to the planetary cycles proposed in the MGC-PC model (Section 4.8).

4.7. Paleontology and Evolution of Life

Speculatively, the MGC-PC cycle (see Section 4.8) provides a theoretical framework to explaining temporal variations in the number of days per year. These variations would result from orbital reconfigurations, changes in axial tilt and rotation, and progressive reduction in solar irradiation and an increase in both gravity and magnetic field intensity. Other possible effects include the reconfiguration of atmospheric pressure, the expansion of the planetary surface, variations in ocean volume, and oscillations in oceanic chemistry and atmospheric composition.

These transformations would be followed by a rise in global temperature and a chaotic environmental phase, eventually leading to relative stabilization. Life would then proceed from the surviving species, adapting—or not—to the new habitats in the oceans, on land, and in the air, while new tectonic plates began to exert their effects on the surface. This may have been linked to changes in biological defense mechanisms against radiation and predation, as well as in strategies for obtaining food.

The evolution of life appears to have occurred in phases of relative stability separated by radical environmental transformations. Interestingly, life first emerged in the oceans, initially in microbial forms, later multicellular, and finally diversified during the Cambrian Explosion. Subsequently, plants expanded onto the continents, with primitive vegetation followed by early forests, accompanied by the first amphibians (~450–350 Ma). Later periods consolidated the development of forests and terrestrial fauna, while the seas hosted aquatic reptiles of the Paleozoic (~350–250 Ma). The period between ~250 and 66 Ma marked the dominance of dinosaurs on land, culminating in the event that led to the current environment.

The immediate impacts of the energie released during an MGC-PC event, as well as their long-term effects, can be grouped into three main categories:

(i) Geophysical – an increase in magnetic field strength and gravity, with a consequent reduction in solar radiation intensity;
(ii) Physical geography – reconfiguration of Earth's surface with redistribution of emerged and submerged areas;
(iii) Atmospheric – increase in atmospheric mass, particularly the recomposition of gases.

Studies suggest that low CO_2 levels, combined with high O_2 concentrations favored the emergence of complex organisms and the development of larger brains, directly influencing the degree of intelligence achieved by different lineages (Bardi, 2025).

These transformations alter ecological strategies, promote the emergence of new life forms, and can render old adaptations obsolete—for instance, the increase in gravity may hinder certain hunting and predation strategies. Future studies are needed to develop mathematical models that explore the correlations between life's evolutionary processes and the geophysical, geological, and geomorphological characteristics proposed by the MGC-PC cycle.

4.8. Astronomy and Planetary Sciences: Cycles of Geodynamic, Orbital, and Climatic Transformations in Earth's Evolution

This section describes Earth’s internal and orbital evolution across eight cycles of planetary coupling, which supposedly occurring over the last two billion years. In this framework, Earth would have evolved from a protoplanet with a mass comparable to Eris to its present stabilized configuration. The number of cycles depends on the initial masses of the protoplanets that formed the present inner planets. Considering that the initial protoplanets had masses between 0.7 and 1.5 times that of Eris, there would be eight cycles for Earth and Venus, and five, four and two cycles for Mars, Mercury, and the Moon, respectively.
Therefore, 564 celestial bodies orbiting the Sun in the inner region.

Figure 4—Planetary Coupling Cycle Diagram (MGC-PC) —illustrates the sequence of fusion events, together with geophysical data and the main temporally associated geological events. The proposed sequence integrates astronomical, geophysical, geological, tectonic, biological, and paleontological records; however, synchronization among these milestones (Figure 4(c)) remains preliminary and requires validation through high-resolution geochronology. Likewise, analyses of the number of days throughout geological time in sedimentary and fossil records, combined with the identification of Milankovitch cycles in the Proterozoic record (Meyers and Malinverno, 2018), would further refine this temporal framework.

Studies indicate that gravitational interactions resulted in orbital migration, collisions, satellite capture, and the ejection of small bodies (Ipatov, 2024; Marov et al., 2023; Kane et al., 2021; Marov, 2018; Grinin, 2017). Rabago et al. (2019) and Taylor et al. (2024) show that gravitational interactions and resonances, when combined with non-gravitational accelerations, can destabilize lunar systems and small-body trajectories, leading to planetary ejection, rotational disruption, collisions, or orbital redistribution of satellites. Blanc et al. (2025) identify mechanisms for the origin of satellites, with particular emphasis on the capture of heliocentric bodies.

Applying the Mutual Gravitational Capture (MGC) model to the evolution of the inner bodies, it is observed that in the early stages, planets were smaller and the energy of encounters was lower. These parameters favored the temporary capture of satellites and the ejection of comets. Furthermore, satellites may have been captured and later destabilized by the approach of another protoplanet. In this context, it can be speculated that the impact of a satellite the size of Deimos could have generated structures comparable to large craters such as Chicxulub. It is also plausible that the minor extinction around ~483 Ma and the mass extinction at ~201 Ma were triggered by the fall of unstable satellites displaced by gravitational encounters..

This mechanism, at low-mass stages, may also have played a role in the capture and stabilization of the Moon. Accordingly, lunar gravitational capture may have occurred only between ~750 and 66 Ma, with its orbit gradually circularized through interactions with nearby protoplanets. During this interval, Earth would have had a mass greater than the Moon's but less than half of its present value. The proposal is that Earth's mass could have ranged between ~48% and 2.5% of its current value, with intermediate stages of 23%, 11%, and 5.3%, such that gravitational interactions would have operated at reduced intensity, with low energy levels.

Beyond the Moon, similar mechanisms may be applied to interpret regional processes such as the origin of the asteroid belt. Chambers (2004) suggested that "something went wrong" in the asteroid belt. Within the MGC-PC framework, it can be speculated that planetary evolution was nearly successful, culminating in the formation of two protoplanets of about 1.5 times the mass of Ceres. A collision between them, at orbital velocities typical of the region (~18 km/s), nearly twenty times the local escape velocity (<1 km/s), would have been sufficiently destructive to fragment them, giving rise to the present asteroid belt. Simulations can test whether bodies of this scale could eject comets with an efficiency comparable to that attributed to Jupiter's gravitational influence, while crater studies and geochemical analyses may assess the plausibility of this hypothesis.

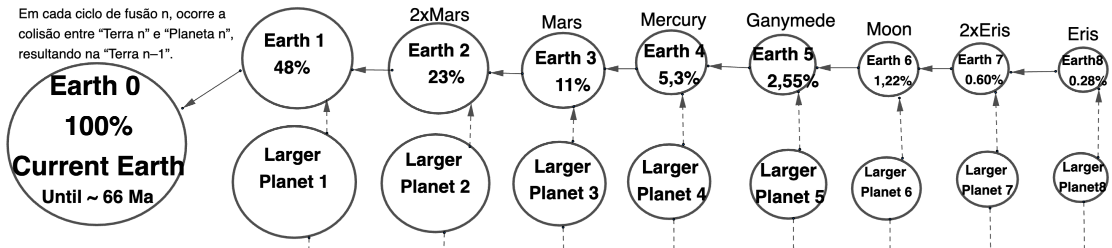

Figure 4 (a): the planetary evolution timeline

Time span of existence eartyh (i) ===>	~270-250Ma to ~66Ma	~380-360Ma to ~270-250Ma	~450-440Ma to ~380-360Ma	~550-540Ma to ~450-440Ma	~750Ma to ~550-540Ma	~1,2Ma to ~750Ma	~2,2-1,8Ga to ~1,2Ga	~4,5Ga to ~2,2-1,8Ga
Mass ratio 48% x 52% => Result:	Earth(i=1)+ Planet(i=1)	Earth(i=2) + Planet(i=2)	Earth(i=3) + Planet(i=3)	Earth(i=4) + Planet(i=4)	Earth(i=5) + Planet(i=5)	Earth(i=6) + Planet(i=6)	Earth(i=7) + Planet(i=7)	Earth(i=8) + Planet(i=8)
Mass smaller planet (i) x current Earth	48.00%	23%	11%	5.3%	2.55%	1.22%	0.60%	0.28%
Densidade Earth (i)	5,20E+03	4,88E+03	4,53E+03	4,18E+03	3,93E+03	3,43E+03	3,33E+03	3.09E+03
Mass Earth (i) smaller planet	2.87E+24	1.38E+24	6.61E+23	3.17E+23	1.52E+23	7.30E+22	3.51E+22	1.68E+22
Mass larger planet (i)	3.11E+24	1.49E+24	7.16E+23	3.43E+23	1.65E+23	7.91E+22	3.80E+22	1.82E+22
Resultant mass: Earth (i-1)	5.97E+24	2.87E+24	1.38E+24	6.60E+23	3.17E+23	1,52E+23	7.30E+22	3.51E+22
Resultant volume: Earth (i-1) - km	1.08E+12	5.51E+11	2.82E+11	1.46E+11	7.58E+10	3,87E+10	2.13E+10	1.05E+10
Resultant surface: Earth (i-1) - km²	5.10E+08	3.25E+08	2.08E+08	1.34E+08	8.67E+07	5.53E+07	3.72E+07	2.33E+07
Maximum ancient cratons: Earth (0)	32%	20%	13%	8,5%	5,4%	3,6%	2,5%	1,5%
Resultant radius: Earth (i-1)	6,371	5,087	4,068	3,265	2,626	2,098	1,720	1,360
Radius of smaller planet (i)	5,087	4,068	3,265	2,626	2,098	1,720	1,360	1,092
Radius of larger planet (i)	5,224	4,178	3,353	2,697	2,155	1,766	1,397	1,121
Gravitational force Earth (i-1)	9.82	7.39	5,55	4.14	3.07	2.31	1.65	1.26
Escape velocity Earth (i) - km/s	8.67	6.72	5.20	4.01	3.11	2.38	1.85	1.43
Escape velocity larger planet (i) - km/s	8.91	6.90	5.34	4.12	3.20	2.45	1.90	1.47
Escape velocity of the system - km/s	8.79	6.81	5.27	4.07	3.15	2.41	1.88	1.45
System Impact Velocity - km/s, n=1	8.79	6.81	5.27	4.07	3.15	2.41	1.88	1.45
System Impact Velocity - km/s, n=0,8	7.86	6.09	4.71	3.64	2.82	2.16	1.68	1.30
Radius Hill Earth (i) - km	1,170,885	916,772	717,825	562,025	440,050	344,548	269,772	211,224
Radius Hill larger planet (i) - km	1,202,545	941,561	737,201	577,222	451,949	353,864	277,066	216,936

Figure 4 (b): the numerical data

Event (1) – ~66 Ma Fusion: Earth 1 + Planet 1 = Current Earth	**Event (2) – ~270–250 Ma** Earth 2+Planet 2=Earth 1 (mass≈2xMars)	**Event (3) – ~380–360 Ma** Fusion: Earth 3 + Planet 3 = Earth 2 (mass≈Mars)
Detailed in sections 4.1 to 4.7 .Core and Magnetic Anomalies .Mantle heterogeneity .Orogenic processes, crustal restructuring and geodynamic implications .Petroleum and mineral reserves .Biological evolution, extinctions .Varve-type sedimentary rocks, tidal rhythmites, and shell fossils	·Permian extinction ~252 Ma .Uralian orogeny with final subduction around ~250 Ma (Puchkov,2009; Puchkov,1997) .Oblique collision between Laurentia and Gondwana ~320–270 Ma, resulting in the Alleghanian orogeny (Hopper et al.,2017) .Opening of the Meso-Tethys Ocean ~280 Ma and the Neo-Tethys Ocean ~230 Ma (Metcalfe,2013) .Subduction of the Paleo-Pacific plate ~260–250 Ma (Allen,2025) .Triassic–Jurassic extinction (~201 Ma) .Fossils ~84 Ma, 370 days per year (de Winter et al.,2020) .Subtropical forests and natural wildfires in North Africa ~84 Ma (Atfy et al.,2016)	·Subtropical forests and natural wildfires in North Africa ~84 Ma (Atfy et al., 2016) .Devonian extinction ~372–359 Ma (Montañez, 2022) .Uralian orogeny (~380 Ma): subduction of the Paleo-Uralian Ocean, collision of the Kazakh block with the Siberian craton (~320–280 Ma) (Puchkov, 2009; Puchkov, 1997) .Opening of the Paleo-Tethys Ocean ~380 Ma (Metcalfe, 2013) .Diversification of vascular plants ~375–359 Ma (Kenrick and Crane, 1997; Morris et al., 2018) .Expansion of the first large trees ~359 Ma (Wohl, 2013) .Decline aquatic vertebrates and abrupt climate changes (Kaiser et al., 2016).
Event (4) – ~450–440 Ma Earth 4+Planet 4=Earth 3 (mass≈Mercury)	**Event (5) – ~550–540 Ma** Earth 5+Planet 5=Earth 4 (mass≈Ganymede)	**Event (6) – ~750 Ma** Earth 6+Planet 6=Earth 5 (mass≈Moon)
·Ordovician–Silurian extinction ~443 Ma ·Closure of the Iapetus Ocean ~430–420 Ma and Caledonian orogeny (Corfu et al.,2014; Corfu et al.,2015; Gee et al.,2008) .Inner core radius ~40% of present Earth, close to ~50% estimated by Zhou et al. (Zhou et al.,2022)	·Cambrian Explosion ~541 Ma (Zhang and Shu,2013) .Very weak geomagnetic field ~550 Ma and regenerated ~550 Ma (Zhou et al.,2022) .Fragmentation of the supercontinent Pannotia ~625–550 Ma (Nance and Murphy,2019) .Formation Iapetus Ocean ~600–500 Ma (Corfu et al.,2014)	·Breakup Rodinia ~750 Ma (Nance and Murphy,2019; Bond,1984) ."Snowball Earth" glaciations ~717–635 Ma and ~584–579 Ma, low geodynamic activity, atmospheric changes, variations in insolation (Casado,2021) .Tidal records around ~620 Ma indicate a solar year of ~400 ± 7 days (Mazumder,2004; Williams,1998).
Event (7) – ~1.2 Ga Earth 7+Planet 7=Earth 6 (mass≈2xEris)	**Event (8) – ~2.2–1.8 Ga** Earth 8+Planet 8=Earth 7 (mass≈Eris)	
·Dissolution of the Columbia supercontinent ~1.2 Ga, lithosphere–mantle reorganization and ~90° rotation of the North China Craton (Liu et al.,2024; Roberts,2013)	·Fragmentation of Kenorland ~2450–1850 Ma, early formation of the Huronian Basin and the Animikie Basin (Young,2015). ·Tidal rhythm records ~2450–1650 Ma indicate 384–435 days per year (Williams,2000; Mazumder,2004).	

Figure 4 (c): the geological events

Water cycle in Earth's evolutionary cycle: Provisionally, the MGC-PC model suggests that the transfer of liquid water between fused planets may have influenced the average depth of the oceans and the proportion of emergent land through time. Large volumes of oceanic water may have been buried during fusion events, interacting within interface zones between the merging bodies. Smaller planets would have had reduced surface areas and a lower capacity to incorporate water into the mantle during fusion. In early stages, protoplanets may have contained either less or more liquid water, depending on their origins, in some cases, entire worlds may have been covered by oceans. In this context, the cycle proposed in Figure 4 allows speculation on water dynamics and the interpretation of evidence related to deep heterogeneities and hydrothermal fluxes. This cycle also provides a framework for evaluating conditions that favored the onset of marine life, the expansion of the first plants, and the establishment of terrestrial animals.

The presence of water within the Earth's interior is observed in the transition zone, with estimated volumes exceeding that of the oceans (Pearson et al., 2014; Gu et al., 2022; Huang et al., 2005; Hallis et al., 2015). Variations in mean sea level have been recorded over the past 540 million years (van der Meer et al., 2025). These variations may reflect a dynamic relationship between the volume and the surface area occupied on the planet through each geological time interval.

Over the past 540 million years, complete cycles of continental assembly and breakup have been identified, accompanied by recurring episodes of global warming and cooling. These variations are evidenced by changes in sea level, the extent of continental flooding, the successive reorganization of lithospheric margins, and isotopic and oceanic records (Kocsis and Scotese, 2021; Scotese et al., 2021). Although occurring at different times, the cycle proposed by Kocsis and Scotese and the MGC-PC model both describe planetary reorganization processes that result in large-scale changes in surface configuration and crustal dynamics.

In addition, an increase in ocean water temperature between approximately 60 and 40 Ma, followed by a progressive cooling, was observed by Rohling et al. (2024). A proposed MGC-PC event around ~66 Ma could have warmed ocean waters through direct contact with exposed mantle. Water has accompanied Earth since its earliest stages. Analyses of enstatite chondrite (EC) meteorites indicate the presence of large amounts of hydrogen from the planet's original formation, suggesting that the internal water reservoir may have been substantial since the earliest stages (Barrett et al., 2025).

4.9. Astronomy and Planetary Sciences: Evidence of MGC-PC on Venus, Mars, and Mercury

Certain structural and orbital features of the other inner planets may represent remnants of past planetary fusion events, such as large mountains, plains, and basins. Studies suggest that Venus may have maintained a habitable climate until about 700 Ma (Way et al., 2016) and that its crust was resurfaced between 700 and 300 Ma (Strom et al., 1994), Schaber et al., 1992). In addition, the occurrence of volcanic plumes containing water vapor may be associated with the release of interior volatiles (Dias et al., 2025). Recent studies attribute its retrograde rotation to atmospheric tides and core–mantle friction rather than giant impacts (Correia and Laskar, 2001)). Mars is characterized by hemispheric dichotomy, crustal variations, and magnetic contrasts. Valantinas et al. (2025) confirm the presence of ferrihydrite, formed in cold and humid environments, and point to indirect evidence of episodic, dynamic, and global events in Mars' geological past.

4.10. Model Limitations and Potential Contributions of the MGC-PC Hypothesis

The literature highlights open questions regarding the evolutionary pathways of the planets in the Solar System. In this context, although speculative in some respects, the MGC-PC hypothesis emerges as a unifying approach to planetary collisions and mergers, consistent with observed physical and isotopic evidence (Table 2).

Table 2. Comparison between Conventional Models and the MGC-PC Hypothesis

Aspect	Conventional Models	MGC-PC Hypothesis
Fusion of differentiated bodies	Partial or destructive collisions not predicted	Core mechanism of complete fusion of planetary bodies
Internal structural recomposition	Absent or rarely considered	Explains coalescence and reassembly of planetary layers
Internal heterogeneities	Attributed to chemical evolution	Explains mantle heterogeneities, ULVZs, water, and organic matter
Magnetic field	Linked to core cooling	Fusion/reorganization of cores, multiple dipoles
Mass extinctions	Consequences without clearly defined cause	Defines causes, including gravitational influence
Crustal profile	Isolated process analysis	Integrated analysis of crustal morphology
Mineral deposits	Volcanism and water transport	Unique transport of soluble and insoluble elements
Petroleum origin	Biogenic or abiogenic	Organic matter from extinctions, trapped in mantle and oceans
Satellites and comets	Impacts or co-accretion	Gravitational capture and ejection
Interdisciplinary integration	Limited to specific domains	Integrates geodynamics, paleontology, astrobiology
Deep geochemical anomalies	Rare plume leaks	Homogeneous core-mantle mixing during fusion
Fossils and sedimentary rocks	Small orbital variations within stable orbits	Sedimentary cycles and climatic changes post-fusion.

Limitations of the MGC-PC model: The morphological signatures predicted by this model, as well as their correlation with observable evidence in the inner planets, depend on validating the impact velocity together with the planetary mass fusion process. The analysis does not include material loss, chemical composition, mantle viscosity, or detailed thermal effects. Energy dissipation was considered with a conservative rate of up to 20%, based on previous studies. This rate may vary according to composition, the presence of oceans, and impact angle, although lower values do not affect the subcritical impact condition. Residual orbital differences were not evaluated.

The results were obtained using simple analytical models developed in Excel spreadsheets, based on Newton's and Kepler's laws. The model assumed that the bodies were initially at rest relative to each other, and from their masses, gravity, velocities, radii, and densities. In this study, computational simulations based on N-body or SPH methods (e.g., REBOUND, GADGET-2, or pkdgrav) were not performed.

However, such tools may not yet incorporate the initial conditions assumed in this study, which require parameters associated with mutual gravitational capture within the Hill sphere. This approach allows exploration of subcritical velocity regimes and collision–fusion scenarios distinct from those typically simulated.

5. Conclusion

The proposed model is at once disruptive, challenging established assumptions; integrative, simultaneously considering astronomy and the geosciences; and complementary to existing theories. It extends classical models by analyzing non-destructive collisions of planetary bodies predicted by astronomy and by proposing the process of mass fusion, emphasizing its enduring morphological signatures.

The hypothesis introduces an innovative perspective on the growth of rocky planets, suggesting that they doubled their mass through successive fusion events, during which the mantle of the smaller body spreads over the larger one, partially preserving its crust. The resulting signatures include mantle heterogeneities, inner core growth, magnetic anomalies, internal boundary zones, orbital variations, mass extinctions, and orogeny. The hypothesis also suggests a solid multi-spherical inner core immersed in a liquid medium, including water, as a possible explanation for observed anomalies in Earth's core.

Earth may have undergone eight MGC-PC events over the past 2 billion years, the most recent occurring around 66 Ma, with an estimated impact velocity of 7.86 km/s, below the escape velocity of 8.79 km/s. Under these conditions, a non-destructive fusion with partial preservation is supported by multidisciplinary evidence. Its validation can be confirmed through comprehensive simulations and supported by future research focusing on the following key areas:

- Numerical simulations of mutual gravitational capture within the Hill sphere, analyzing the influence of varying masses, angles, and orbital velocity differences between bodies at the moment of impact;
- Seismic modeling to detect a composition resulting from multiple internal spheres, variations in their shape, and the aggregation of iron, liquid iron–nickel, and water under high pressure within the inner core;
- Identify the compatibility of heterogeneities associated with the mixing of mantle material, the outer core, and the planet's buried crust with hotspots (including Yellowstone), the South Atlantic Magnetic Anomaly (SAMA), mantle plumes, as well as LLSVPs and ULVZs;
- High-pressure interactions among water, volatiles, organic matter, and buried crust within the interface zone as potential sources of hydrocarbons and hydrogen;
- Integrated reinterpretation of tectonic cycles, orogenic processes, mineral deposition, and mass extinctions in light of MGC-PC events and their orbital effects.

In summary, the MGC hypothesis proposes a conceptual reorganization based on testable evidence, opening new perspectives for understanding planetary evolution and requiring future validation through mathematical models and comparison with geological and orbital records.

The limitations of current models are widely acknowledged in studies of orbital evolution and planetary mass dynamics, and each of them can, in its own way, incorporate the new parameters offered by the MGC-PC model. The methodological limitations of the present study do not compromise the proposed analysis of planetary fusion or the correlation of its morphological signatures with the broad range of geophysical, geochemical, and astronomical evidence already examined by science. Thus, these methodological constraints do not undermine the physical consistency of the MGC-PC.

Acknowledgments

This article is dedicated, with deep respect, to the late Dimas Candido Waltrick, whose conviction that the Pacific Ocean represents an impact crater inspired the beginning of this journey.

The author thanks Charlesworth Author Services for their editorial assistance and the anonymous reviewers for their valuable comments in the version preceding the initial preprint publication.

I extend my gratitude to the researchers who made their findings publicly available, whom I consider true mentors from a distance, as well as to those with whom I had the opportunity to clarify specific questions. In particular, to those who kindly shared their opinions and results, which were an important light in my reflections.

Data Availability: All relevant data are available within the article.

Competing Interests: The author declares no competing interests.

Funding: No external funding was received for this work.

Generative AI and AI-assisted technologies statement: During the preparation of this work, the author used ChatGPT (OpenAI) to support language refinement, translation, and improvement of clarity. After using this tool, the author reviewed and edited the content as necessary and takes full responsibility for the content of this publication.

References

Allen MB, Song S, Wang C. 2025 An invasion model for the start of Paleo-Pacific subduction. Geology 53, 488–492, https://doi.org/10.1130/G53022.1

Atfy HE, Sallam H, Jasper A, Uhl D. 2016 The first evidence of paleo-wildfire from the Campanian (Late Cretaceous) of North Africa. Cretaceous Research 57, 306–310, https://doi.org/10.1016/j.cretres.2015.09.012

Asphaug E. 2014 Impact origin of the Moon? Annual Review of Earth and Planetary Sciences. 42, 551–578 https://doi.org/10.1146/annurev-earth-050212-124057

Asphaug E, Agnor CB, Williams Q. 2006 Hit-and-run planetary collisions. Nature 439, 155–160, https://doi.org/10.1038/nature04311

Bardi U. 2025 The Role of Carbon Dioxide in the Evolution of Intelligence: Solving the Dinosauroid Question. *Qeios*. https://doi.org/10.32388/IKNUZU

Barrera E, Savin SM. 1999 Evolution of late Campanian-Maastrichtian marine climates and oceans. In Evolution of the Cretaceous Ocean-Climate System. Geological Society of America; Special Paper 332, 245–282, https://doi.org/10.1130/0-8137-2332-9.245

Barrett TJ, Bryson JFJ, Geraki K. 2025 The source of hydrogen in earth's building blocks. Icarus 436, 116588, https://doi.org/10.1016/j.icarus.2025.116588

Berezhnaya ED, Dubinin AV. 2017 Determination of the platinum-group elements and gold in ferromanganese nodule reference material NOD-A-1. Geochemistry International, 55, 218-224, https://doi.org/10.1134/S0016702917010037

Biggin AJ, Steinberger B, Aubert J, Suttie N, Holme R, Torsvik TH. et al. 2012 Possible links between long-term geomagnetic variations and convection processes of the entire mantle. Nature Geoscience 5, 526–533, https://doi.org/10.1038/ngeo1521

Bizzarro M, Johansen A, Dorn C. 2025 The cosmochemistry of planetary systems. Nature Reviews Chemistry, 9, 378-396 https://doi.org/10.1038/s41570-025-00711-9

Blanc M, Crida A, Shibaike Y, Charnoz S, El Moutamid M, Estrada P. et al. 2025 The formation of Saturn's regular satellites: From circumplanetary disk to orbital architecture. Space Science Reviews, 221, Article 56. https://doi.org/10.48550/arXiv.2503.01351

Bond GC, Nickeson PA, Kominz MA. 1984 Breakup of a supercontinent between 625 Ma and 555 Ma: new evidence and implications for continental histories. Earth Planet. Sci. Lett. 70, 325-345, https://doi.org/10.1016/0012-821X(84)90017-7

Brenker FE, Vincze L, Vekemans B, Nasdala L, Stachel T, Vollmer C. et al. 2005 Detection of a Ca-rich lithology in the Earth's deep (> 300 km) convecting mantle. Earth Planet. Sci. Lett. 236, 579–587, https://doi.org/10.1016/j.epsl.2005.05.021

Brusatte SL, Butler RJ, Barrett PM, Carrano MT, Evans DC, Lloyd GT, et al. 2015 The extinction of the dinosaurs. Biological Reviews 90, 628–642, https://doi.org/10.1111/brv.12128

Canup RM. 2004 Simulations of a late lunar-forming impact. Icarus 168, 433–456, https://doi.org/10.1016/j.icarus.2003.09.028

Canup RM, Asphaug E. 2001 Origin of the Moon in a giant impact near the end of the Earth's formation. Nature 412, 708-712, https://doi.org/10.1038/35089010

Casado JA. 2021 A Review of Neoproterozoic Global Glaciations and a Biotic Cause of Them. Earth Systems and Environment, 5, 811–824, https://doi.org/10.1007/s41748-021-00258-x

Chambers JE. 2004 Planetary accretion in the inner Solar System. Earth Planet. Sci. Lett. 223, 241-252 https://doi.org/10.1016/j.epsl.2004.04.031

Collins GS, Melosh j, Osinsk GR. 2012 The impact-cratering process. Elements 8, 25–30, https://doi.org/10.2113/gselements.8.1.25

Corfu F, Andersen TB, Gasser D. 2015 The Scandinavian Caledonides: main features, conceptual advances and critical questions. Geological Society London 390, 9-43, https://doi.org/10.1144/SP390.25

Corfu F, Gasser D, Chew DM. 2014 New perspectives on the Caledonides of Scandinavia and related areas: introduction. Geological Society 390, 1–8, https://doi.org/10.1144/SP390.28

Correia ACM, Laskar J. 2001 The four final rotation states of Venus. Nature 411, 767–770, https://doi.org/10.1038/35081000

Courtillot VE, Renne PR. 2003 On the ages of flood basalt events. Comptes Rendus Geoscience 335, 113–140, https://doi.org/10.1016/S1631-0713(03)00006-3

Crossley SD, Setera JB, Anzures BA, Iacovino K, Buckley WP, Eckley SA, et al. 2025 Percolative sulfide core formation in oxidized planetary bodies. Nature Communications, 16, 3233, https://doi.org/10.1038/s41467-025-58517-8

Cuk M, Stewart ST. 2012 Making the moon from a fast-spinning Earth: A giant impact followed by resonant despinning. Science 338, 1047–1052, https://doi.org/10.1126/science.1225542

Dannberg J, Gassmoeller R, Thallner D, LaCombe F, Sprain C. 2023 Changes in core-mantle boundary heat flux patterns throughout the supercontinent cycle. Geophysical Journal International 237, 1251–1274, https://doi.org/10.1093/gji/ggae075

de Winter NJ, Goderis S, van Malderen SJM, Sinnesael M, Vansteenberge S, Snoeck C, et al. 2020 Subdaily-scale chemical variability in a Torreites sanchezi rudist shell: Implications for rudist paleobiology and the Cretaceous day–night cycle. Paleoceanography Paleoclimatology, 35, e2019PA003723, https://doi.org/10.1029/2019PA003723

Dean CD, Chiarenza AA, Doser JW, Farnsworth A, Jone LA, et al. 2025 The structure of the end-Cretaceous dinosaur fossil record in North America. Current Biologu 35, p1973-1968.E6, https://doi.org/10.1016/j.cub.2025.03.025

Denman TR, Leinhardt ZM, Carter PJ. 2022 Atmosphere loss in oblique Super-Earth collisions. Monthly Notices of the Royal Astronomical Society 513, 1680–1700, https://doi.org/10.1093/mnras/stac923

Deuss A. 2014 Heterogeneity and Anisotropy of Earth's Inner Core. Annual Review of Earth and Planetary Sciences, 42, 103-126. https://doi.org/10.1146/annurev-earth-060313-054658

Dias JA, Machado P, Robert S, Erwin J, Lefèvre M, Wilson CF, et al. 2025 Volcanic gas plumes' effect on the spectrum of Venus. Icarus 438, 116589, https://doi.org/10.1016/j.icarus.2025.116589

Emsenhuber A, Cambioni s, Asphaug E, Gabriel TSJ, Schwartz SR, Furfaro R. 2020 Realistic on-the-fly outcomes of planetary collisions. II. Bringing machine learning to N-body simulations. The Astrophysical Journal 891, 6, https://doi.org/10.3847/1538-4357/ab6de5

Emsenhuber A, Asphaug E. 2019 Graze-and-merge collisions under external perturbers. The Astrophysical Journal 881, 102, https://doi.org/10.3847/1538-4357/ab2f8e

Feng J, Yao H, Wang Y, Poli P, Mao Z. 2021 Segregated oceanic crust trapped at the bottom mantle transition zone revealed from ambient noise interferometry. Nature Communications 12, 2531, https://doi.org/10.1038/s41467-021-22853-2

Finlay CC, Kloss C, Olsen N, Hammer MD, øffner-Clausen L, Grayver A. et al. 2020 The CHAOS-7 geomagnetic field model and observed changes in the South Atlantic Anomaly. Earth Planets and Space 72, 156, https://doi.org/10.1186/s40623-020-01252-9

Fischer-Gödde M, Tusch J, Goderis S, Bragagni A, Mohr-Westheide T, Messling N. et al. 2024 Ruthenium isotopes show the Chicxulub impactor was a carbonaceous-type asteroid. Science 385, 752–756, https://doi.org/10.1126/science.adk4868

Fouquet Y, Auclair G, Cambon P, Etoubleau J. 1988 Geological setting and mineralogical and geochemical investigations on sulfide deposits near 13°N on the East Pacific Rise. Marine Geology 84, 145-178, https://doi.org/10.1016/0025-3227(88)90098-9

Gee DG, Fossen H, Henriksen N, Higgins AK. 2008 From the Early Paleozoic Platforms of Baltica and Laurentia to the Caledonide Orogen of Scandinavia and Greenland. Episodes 31, 44-51, https://doi.org/10.18814/epiiugs/2008/v31i1/007

Genda H, Kokubo E, Ida S. 2012 Merging criteria for giant impacts of protoplanets. The Astrophysical Journal 744, 137, https://doi.org/10.1088/0004-637X/744/2/137

Genda H, and Abe Y. 2005 Enhanced atmospheric loss on protoplanets at the giant impact phase in the presence of oceans. Nature 433, 842–844, https://doi.org/10.1038/nature03360

Greenough JD, Kamo SL, Davis DW, Larson K, Zhang Z, Layton-Matthews D. et al. 2021 Old subcontinental mantle zircon below Oahu. Communications Earth and Environment 2, 189, https://doi.org/10.1038/s43247-021-00261-0

Grinin LE. 2017 Evolution of the Early Solar System in Terms of Big History and Universal Evolution. Journal of Big History, 2, 15–26, https://doi.org/10.22339/jbh.v2i1.2252

Gu T, Pamato MG, Novella D, Alvaro M, Fournelle J, Brenker FE. et al. 2022 Hydrous peridotitic fragments of Earth’s mantle 660 km discontinuity sampled by a diamond. Nature Geoscience 15, 950–954, https://doi.org/10.1038/s41561-022-01024-y

Hallis LJ, Huss GR, Nagashima K, Taylor GJ, Halldórsson SA, Hilton DR. et al. 2015 Evidence for primordial water in Earth’s deep mantle. Science 350, 795–797, https://doi.org/10.1126/science.aac4834

Hansen SE, Garnero EJ, Li M, Shim SH, Rost S. 2023 Globally distributed subducted materials along the Earth’s core-mantle boundary: Implications for ultralow velocity zones. Science Advances 9, eadd4838, https://doi.org/10.1126/sciadv.add4838

He Y, Sun S, Kim DY, Jang BG, Li H, Mao HK. 2022 Superionic iron alloys and their seismic velocities in Earth's inner core. Nature 602, 258–262, https://doi.org/10.1038/s41586-021-04361-x

Hein FJ, Cotterill DK. 2006 The Athabasca Oil Sands – A regional geological perspective, Fort McMurray area, Alberta, Canada. Natural Resources Research 15, 85–102, https://doi.org/10.1007/s11053-006-9015-4

Hoke GD, Garzione CN. 2008 Paleosurfaces, paleoelevation, and the mechanisms for the late Miocene topographic development of the Altiplano plateau. Earth Planet. Sci. Lett. 271, 192–201, https://doi.org/10.1016/j.epsl.2008.04.008

Höök M, Bardi U, Feng L, Pang X. 2010 Development of oil formation theories and their importance for peak oil. Marine and Petroleum Geology 27, 1995-2004, https://doi.org/10.1016/j.marpetgeo.2010.06.005

Hopper E, Fischer KM, Wagner LS, Hawman RB. 2017 Reconstructing the end of the Appalachian orogeny. Geology 45, 15–18, https://doi.org/10.1130/G38453.1

Hu S, Ji J, Richardson DC, Zhao Y, Zhang Y. 2018 The formation mechanism of 4179 Toutatis' elongated bilobed structure in a close Earth encounter scenario. Monthly Notices of the Royal Astronomical Society 478, 501–515, https://doi.org/10.1093/mnras/sty1073

Huang X, Xu Y, Karato S. 2005 Water content in the transition zone from electrical conductivity of wadsleyite and ringwoodite. Nature 434, 746–749, https://doi.org/10.1038/nature03426

Ipatov SI. 2024 Migration of Celestial Bodies in the Solar System and in Some Exoplanetary Systems. Solar System Research, 58, S50-S63, https://doi.org/10.1134/S0038094623600105

Jagoutz O, Bouilhol P, Schaltegger U, Müntener O. 2019. The isotopic evolution of the Kohistan–Ladakh arc from subduction initiation to continent–arc collision. Geological Society, London, Special Publications 483, 165–182, https://doi.org/10.1144/SP483.7

Javoy M, Kaminski E. 2014 Earth's Uranium and Thorium content and geoneutrinos fluxes based on enstatite chondrites. Earth Planet. Sci. Lett. 407, 1-8, https://doi.org/10.1016/j.epsl.2014.09.028

Jutzi M, Benz W. 2016 Formation of bi-lobed shapes by sub-catastrophic collisions: A late origin of comet 67P/C-G's structure. Astronomy and Astrophysics 597, A62, https://doi.org/10.1051/0004-6361/201628964

Kaiser SI, Aretz M, Becker RT. 2016 The global Hangenberg Crisis (Devonian–Carboniferous transition): review of a first-order mass extinction. Geological Society, London, Special Publications 423, 387-437, https://doi.org/10.1144/SP423.9

Kane SR, Arney GN, Byrne PK, Dalba PA, Desch SJ, Horner J, et al. 2021 The fundamental connections between the Solar System and exoplanetary science. JGR Planets 126, e2020JE006643, https://doi.org/10.1029/2020JE006643

Kegerreis J, Eke V, Catling D, Massey R, Teodoro L, Zahnle K. 2020 Atmospheric erosion by giant impacts onto terrestrial planets: A scaling law for any speed, angle, mass, and density. The Astrophysical Journal Letters 901, L31, https://doi.org/10.3847/2041-8213/abb5fb

Keller G, Mateo P, Monkenbusch J, Thibault N, Punekar J, Spangenberg JE. et al. 2020 Mercury linked to Deccan Traps volcanism, climate change and the end-Cretaceous mass extinction. Global and Planetary Change 194, 103312 https://doi.org/10.1016/j.gloplacha.2020.103312

Keller G. 2012 The Cretaceous–Tertiary mass extinction, Chicxulub impact, and Deccan volcanism. In: Talent JA (ed.) Earth and Life. International Year of Planet Earth. Springer (Livro), Dordrech 759-793 https://doi.org/10.1007/978-90-481-3428-1_25

Kendall JD, Melosh HJ. 2016 Differentiated planetesimal impacts into a terrestrial magma ocean: fate of the iron core. Earth Planet. Sci. Lett. 448, 24–33, https://doi.org//10.1016/j.epsl.2016.05.012

Kenrick P, Crane PR. 1997 The origin and early evolution of plants on land. Nature 389, 33-39, https://www.nature.com/articles/37918

Kocsis AT,and Scotese CR. 2021 Mapping paleocoastlines and continental flooding during the Phanerozoic. *Earth-Science Reviews*, 213,103463. https://doi.org/10.1016/j.earscirev.2020.103463

Konyuhov AI and Maleki B. 2006 The Persian Gulf Basin: Geological history, sedimentary formations, and petroleum potential. Lithology and Mineral Resources 4, 344-361, https://doi.org/10.1134/S0024490206040055

Kupenko I, Aprilis G, Vasiukov DM, McCammon C, Chariton S, Cerantola V. et al. 2019 Magnetism in cold subducting slabs at mantle transition zone depths. Nature 570, 102–106, https://doi.org/10.1038/s41586-019-1254-8

Kutcherov VG, Krayushkin VA. 2010 Deep-seated abiogenic origin of petroleum: From geological assessment to physical theory. Reviews of Geophysics 48, RG1001, https://doi.org/10.1029/2008RG000270

Li Y, Zhang X, Xin S, Liu W. 2019 Evolution of Persian Gulf Basin and formation of super-large oil and gas fields. Geology in China, https://doi.org/10.11781/sysydz201904548

Liu B, Jin S, Tian G, Li L, Qin Y, Xie Z, et al. 2024 Mesoproterozoic (ca. 1.3 Ga) A-Type Granites on the Northern Margin of the North China Craton: Response to Break-Up of the Columbia Supercontinent. Minerals 14, 622, https://doi.org/10.3390/min14060622

Long JA, Niedźwiedzki G, Garvey J, Clement AM, Camens AB, Eury CA, et al. 2025 Earliest amniote tracks recalibrate the timeline of tetrapod evolution. Nature, 641,1193–1200, https://doi.org/10.1038/s41586-025-08884-5

Mäkinen AM, Deuss A. 2011 Global seismic body-wave observations of temporal variations in the Earth′s inner core, and implications for its differential rotation. Geophysical Journal International 187, 355–370, https://doi.org/10.1111/j.1365-246X.2011.05146.x

Mazumder R. 2004 Implications of lunar orbital periodicity from the Chaibasa tidal rhythmite (India) of late Paleoproterozoic age. Geology 32, 841–844, https://doi.org/10.1130/G20424.1

Metcalfe I. 2013 Gondwana dispersion and Asian accretion: Tectonic and palaeogeographic evolution of eastern Tethys. Journal of Asian Earth Sciences 66, 1-33, https://doi.org/10.1016/j.jseaes.2012.12.020

Messling N, Willbold M, Kallas L, Elliott T, Fitton JG, Müller T, et al. 2025 Ru and W isotope systematics in ocean island basalts reveals core leakage. Nature 642, 376-380, https://doi.org/10.1038/s41586-025-09003-0

Montañez, IP. 2022 Current synthesis of the penultimate icehouse and its imprint on the Upper Devonian through Permian stratigraphic record. Geological Society, London, Special Publications, 512, 213–245, https://doi.org/10.1144/SP512-2021-124

Morbidelli A, Tsiganis K, Batygin K, Crida A, Gomes R. 2012 Explaining why the uranian satellites have equatorial prograde orbits despite the large planetary obliquity. Icarus 219, 737–740, https://doi.org/10.1016/j.icarus.2012.03.025

Marov M. 2018 The formation and evolution of the Solar System. In Oxford Research Encyclopedia of Planetary Science. Oxford University Press, https://doi.org/10.1093/acrefore/9780190647926.013.2

Marov MY, Ipatov SI. 2023 Migration processes in the Solar System and their role in the evolution of the Earth and planets. Physics–Uspekhi, 66, 2-31, https://doi.org/10.3367/UFNe.2021.08.039044

Meyers SR, Malinverno A. 2018 Proterozoic Milankovitch cycles and the history of the solar system. Proceedings of the National Academy of Sciences 115, 6363-6368, https://doi.org/10.1073/pnas.1717689115

Morris JL, Puttick MN, Clark JW, Edwards D, Kenrick P, Pressel S. et al. 2018 The timescale of early land plant evolution. Proceedings of the National Academy of Sciences of the USA (PNAS), 115, E2274-E2283, https://doi.org/10.1073/pnas.1719588115

Nance RD, Murphy JB. 2019 Supercontinents and the case of Pannotia. Geological Society, London, Special Publications 470, 65-86, https://doi.org/10.1144/SP470.5

Nance RD, Murphy JB, Santosh M. 2014 The supercontinent cycle: A retrospective essay. Gondwana Research 25, 4–29, https://doi.org/10.1016/j.gr.2012.12.026

Neumann V, Ma N, Bouvier A, Trieloff M. 2024 Formação planetesimal recorrente em uma parte externa do início do sistema solar. Scientific Reports 14, 1417, https://doi.org/10.1038/s41598-024-63768-4

Nordstrom DK, McCleskey RB, Ball JW. 2009 Sulfur geochemistry of hydrothermal waters in Yellowstone National Park: IV Acid–sulfate waters. Applied Geochemistry 24, 191–207, https://doi.org/10.1016/j.apgeochem.2008.11.019

Pastor-Galán D, Nance RD, Murphy JB, Spencer CJ. 2019 Supercontinents: myths, mysteries, and milestones. Geological Society, London, Special Publications 470, 39–64, https://doi.org/10.1144/SP470.16

Pearson DG, Brenker FE, Nestola F, McNeill J, Nasdala L, Hutchison MT. et al. 2014 Hydrous mantle transition zone indicated by ringwoodite included within diamond. Nature 507, 221–224, https://doi.org/10.1038/nature13080

Puchkov VN. 2009 The Evolution of the Uralian Orogen. Geological Society, London, Special Publications 327, 161–195, https://doi.org/10.1144/SP327.9

Puchkov VN. 1997 Structure and Geodynamics of the Uralian Orogen. In: Burg, J.P. and Ford, M. (eds) Orogeny Through Time. Geological Society, London, Special Publications 121, 201–236, https://doi.org/10.1144/GSL.SP.1997.121.01.09

Yuan Q, Li M, Desch SJ, Ko B, Deng H, Garnero EJ. et al. 2023 Moon-forming impactor as a source of Earth's basal mantle anomalies. Nature 623, 95–99, https://doi.org/10.1038/s41586-023-06589-1

Rabago I, Steffen JH. 2019 Survivability of Moon Systems Around Ejected Gas Giants. Monthly Notices of the Royal Astronomical Society 489, 2323–2329, https://doi.org/10.1093/mnras/sty2552

Raymond SN. 2024 The Solar System: structural overview, origins and evolution. arXiv preprint (arXiv:2404.14982), https://doi.org/10.48550/arXiv.2404.14982

Raymond SN, Izidoro A, Morbidelli A. 2020 Solar system formation in the context of extrasolar planets. arXiv preprint (arXiv.1812.01033) https://doi.org/10.48550/arXiv.1812.01033

Renne PR, Deino AL, Hilgen FJ, Kuiper KF, Mark DF, Mitchell III WS. et al. 2013 Time scales of critical events around the Cretaceous–Paleogene boundary. Science 339, 684–687, https://doi.org/10.1126/science.1230492

Roberts NMW. 2013 The boring billion? – Lid tectonics, continental growth and environmental change associated with the Columbia supercontinent. Geoscience Frontiers 4, 681-691, https://doi.org/10.1016/j.gsf.2013.05.004

Rohling EJ, Gernon TM, Heslop D, Reichart DJ, Roberts AP, Yu J. 2024 Reconciling the Apparent Discrepancy Between Cenozoic Deep-Sea Temperatures From Proxies and From Benthic Oxygen Isotope Deconvolution. Paleoceanography and Paleoclimatology 39, e2024PA004872, https://doi.org/10.1029/2024PA004872

Rojas-Agramonte Y, Pardo N, van Hinsbergen DJJ, Winter C, Marroquín-Gómez MP, Liu S, et al. 2024 Zircon xenocrysts from Easter Island (Rapa Nui) reveal hotspot activity since the middle Jurassic. AGU Advances 5, e2024AV001351, https://doi.org//10.1029/2024AV001351

Rojas-Agramonte Y, Kaus BJ, Piccolo A, Williams IS, Gerdes A, Wong J. et al. 2022 Zircon dates long-lived plume dynamics in oceanic islands. Geochemistry, Geophysics, Geosystems 23, e2022GC010485, https://doi.org/10.1029/2022GC010485

Rowley DB. 1996 Age of initiation of collision between India and Asia: A review of stratigraphic data. Earth Planet. Sci. Lett. 145, 1–13, https://doi.org/10.1016/S0012-821X(96)00201-4

Savage PS, Moynier F, Chen H, Shofner G, Siebert J, Badro J, et al. 2015 Copper isotope evidence for large-scale sulphide fractionation during Earth's differentiation. Geochemical Perspectives Letters 1, 53–64, https://doi.org/10.7185/geochemlet.1506

Schaber GG, Strom RG, Moore HJ, Soderblom LA, Kirk RL, Chadwick DJ. et al. 1992 Geology and Distribution of Impact Craters on Venus: What Are They Telling Us? Journal of Geophysical Research: Planets, 97, 13257–13301, https://doi.org/10.1029/92JE01246

Scotese CR, Song H, Mills BJW, van der Meer DG. 2021 Phanerozoic paleotemperatures: The Earth's changing climate during the last 540 million years. Earth-Science Reviews, 213, 103503. https://doi.org/10.1016/j.earscirev.2021.103503

Scrutton, CT. 1978 Periodic growth features in fossil organisms and the length of the day and month. Tidal Friction and the Earth's Rotation (Book, Springer) 154–196, https://doi.org/10.1007/978-3-642-67097-8_12)

Seabrook S, Law CS, Thurber AR, Ladroit Y, Cummings V, Tait L. et al. 2025 Antarctic seep emergence and discovery in the shallow coastal environment. Nature Communications. 16, 8740 https://www.nature.com/articles/s41467-025-63404-3

Seymour RS, Lillywhite HB. 2016 Why vascular siphons with sub-atmospheric pressures are physiologically impossible in sauropod dinosaurs. Journal of Experimental Biology, 219, 2078–2080, https://doi.org/10.1242/jeb.137505

Seymour RS. 2016 Cardiovascular Physiology of Dinosaurs. American Physiological Society, https://doi.org/10.1152/physiol.00016.2016

Seymour RS. 2009 Raising the sauropod neck: it costs more to get less. Biology Letters, 5, 317–319, https://doi.org/10.1098/rsbl.2009.0096

Seymour RS, Lillywhite HB. 2000 Hearts, neck posture and metabolic intensity of sauropod dinosaurs. Proceedings of the Royal Society of London. Series B: Biological Sciences 267, 1883–1887, https://doi.org/10.1098/rspb.2000.1225

Sleep NH, Bird DK, Pope E. 2012 Paleontology of the Earth's Mantle. Annu. Rev. Earth Planet. Sci. 40, 277-300, https://doi.org/10.1146/annurev-earth-092611-090602

Snelling EP, Seymour RS. 2024 The hearts of large mammals generate higher pressures, are less efficient and use more energy than those of small mammals. Journal of Experimental Biology, 227, jeb247747, https://doi.org/10.1242/jeb.247747

Strom RG, Schaber GG, Dawson DD. 1994 The Global Resurfacing of Venus. Journal of Geophysical Research: Planets, 99, 10899–10926, https://doi.org/10.1029/94JE00388

Taylor AG, Steckloff JK, Seligman DZ, Farnocchia D, Dones L, Vokrouhlický D. et al. 2024 The dynamical origins of the dark comets and a proposed evolutionary track. Icarus 420, 116207, https://doi.org/10.1016/j.icarus.2024.116207

Torsvik TH, Steinberger B, Ashwal LD, Doubrovine PV, Tronnes RG. 2016 Evolution and dynamics of the Earth – a tribute to Kevin Burke. Canadian Journal of Earth Sciences 53, 1073-1087, https://doi.org/10.1139/cjes-2015-0228

Vaes B, van Hinsbergen DJJ. 2025 Slow True Polar Wander Around Varying Equatorial Axes Since 320 Ma. AGU Advances 6, e2024AV001515, https://doi.org/10.1029/2024AV001515

Valantinas A, Mustard JF, Chevrier V, Mangold N, Bishop JL, Pommerol A, et al. 2025 The detection of ferrihydrite in Martian red dust records ancient cold and wet conditions on Mars. Nature Communications, 16, 1712, https://doi.org/10.1038/s41467-025-56970-z

Valdiya KS. 1984 Evolution of the Himalaya. Tectonophysics 105, 229–248, https://doi.org/10.1016/0040-1951(84)90205-1

van der Meer DG, Stap LB, Scotese CR, Mills BJW, Sluijs A, van Hinsbergen DJJ. 2025 Phanerozoic orbital-scale glacio-eustatic variability. Earth Planet. Sci. Lett. 619, 119526, https://doi.org/10.1016/j.epsl.2025.119526

van Hinsbergen DJJ, Steinberger B, Guilmette C, Maffione M, Gürer D, Peters K. et al. 2021 A record of plume-induced plate rotation triggering subduction initiation. Nature Geoscience 14, 626–630, https://doi.org/10.1038/s41561-021-00780-7 van Hinsbergen DJJ, Torsvik TH, Schmid SM, Maţenco LC, Maffione M, Vissers RLM, et al. 2019 Orogenic architecture of the Mediterranean region and kinematic reconstruction of its tectonic evolution since the Triassic. Gondwana Research 81, 79–229, https://doi.org/10.1016/j.gr.2019.07.009

Vidale JE, Wang W, Wang R, Pang G, Koper KD. 2025 Annual scale variability in both rotation rate and near-surface of the Earth's inner core. Nature Geoscience 18, 267–272, https://doi.org/10.1038/s41561-025-01642-2

Wang J, Lekić V, Schmerr NC, Gu YJ, Guo Y, Lin R. 2024 Mesozoic intraoceanic subduction shaped the lower mantle under the East Pacific uplift. Science Advances 10, eado1219, https://doi.org/10.1126/sciadv.ado1219

Wang W, Vidale JE, Pang G, Koper KD, Wang R. 2024 Inner core backtracking by seismic waveform change reversals. Nature 631, 340–343, https://doi.org/10.1038/s41586-024-07536-4

Way MJ, Del Genio AD, Kiang NY, Sohl LE, Grinspoon DH, Aleinov I, et al. 2016 Was Venus the first habitable world of our solar system? Geophysical Research Letters, 43, 8376-8383, https://doi.org/10.1002/2016GL069790

Wells JW. 1963 Coral growth and geochronometry. Nature 197, 948–950, https://doi.org/10.1038/197948a0

Williams GE. 2000 Geological Constraints on the Precambrian History of Earth's Rotation and the Moon's Orbit. Reviews of Geophysics 38, 37-59, https://doi.org/10.1029/1999RG900016

Williams GE. 1998 Precambrian tidal and glacial clastic deposits: Implications for Precambrian Earth-Moon dynamics and palaeoclimate. Sedimentary Geology 120, 55–74, https://doi.org/10.1016/S0037-0738(98)00027-X

Wohl E. 2013 Floodplains and wood. Earth-Sci. Rev. 123, 194–212, https://doi.org/10.1016/j.earscirev.2013.04.009

Young GM. 2015 Did prolonged two-stage fragmentation of the supercontinent Kenorland lead to arrested orogenesis on the southern margin of the Superior province? Geoscience Frontiers, 6, 410-435, https://doi.org/10.1016/j.gsf.2014.04.003

Zhang XL, Shu DG. 2013 Causes and consequences of the Cambrian explosion. Science China Earth Sciences, 57, 930–942, https://doi.org/10.1007/s11430-013-4751-x

Zhao Y, Ji J, Huang J, Hu S, Hou X, Li Y. et al. 2015 Orientation and rotational parameters of asteroid 4179 Toutatis: new insights from Chang'e-2's close flyby. Monthly Notices of the Royal Astronomical Society 450, 3620–3632, https://doi.org/10.1093/mnras/stv792

Zhong S and Hager BH. 2003. Entrainment of a dense layer by thermal plumes. Journal of Geophysical Research: Solid Earth 108, B5, 2230, https://doi.org/10.1029/2002JB002207

Zhou T, Tarduno JA, Nimmo F, Cottrell RD, Bono RK, Ibanez-Mejia M. et al. 2022 Early Cambrian renewal of the geodynamo and the origin of inner core structure. Nature Communications 13, 4161, https://doi.org/10.1038/s41467-022-31677-7

Figure captions

Figure 1 – Dynamic sequence of planetary merger.

Figure 2 – Steps of the MGC-PC process resulting from Mutual Gravitational Capture (MGC).

Figure 3 – Persistent morphological signatures generated by the MGC process.

Figure 4 – Planetary Coupling Cycle Diagram (MGC-PC)

Tables

Table 1. Comparative scenarios for planetary capture and fusion.

Table 2. Comparison between Conventional Models and the MGC-PC Hypothesis